Single-Molecule Spectroscopy, Imaging, and Photocontrol: Foundations for Super-Resolution Microscopy

Nobel Lecture, December 8, 2014

by W. E. (William E.) Moerner

Departments of Chemistry and (by Courtesy) of Applied Physics
Stanford University, Stanford, California 94305 USA.

ABSTRACT

The initial steps toward optical detection and spectroscopy of single molecules in condensed matter arose out of the study of inhomogeneously broadened optical absorption profiles of molecular impurities in solids at low temperatures. Spectral signatures relating to the fluctuations of the number of molecules in resonance led to the attainment of the single-molecule limit in 1989 using frequency-modulation laser spectroscopy. In the early 90s, many fascinating physical effects were observed for individual molecules, and the imaging of single molecules as well as observations of spectral diffusion, optical switching and the ability to select different single molecules in the same focal volume simply by tuning the pumping laser frequency provided important forerunners of the later super-resolution microscopy with single molecules. In the room temperature regime, imaging of single copies of the green fluorescent protein also uncovered surprises, especially the blinking and photoinduced recovery of emitters, which stimulated further development of photoswitchable fluorescent protein labels. Because each single fluorophore acts a light source roughly 1 nm in size, microscopic observation and localization of individual fluorophores is a key ingredient to imaging beyond the optical diffraction limit. Combining this with active control of the number of emitting molecules in the pumped volume led to the

super-resolution imaging of Eric Betzig and others, a new frontier for optical microscopy beyond the diffraction limit. The background leading up to these observations is described and selected current developments are summarized.

1. THE EARLY DAYS

1.1 Introduction and early inspirations

I want to thank the Nobel Committee for Chemistry, the Royal Swedish Academy of Sciences, and the Nobel Foundation for selecting me for this prize recognizing the development of super-resolved fluorescence microscopy. I am truly honored to share the prize with my two esteemed colleagues, Stefan Hell and Eric Betzig. My primary contributions center on the first optical detection and spectroscopy of single molecules in the condensed phase [1], and on the observations of imaging, blinking and photocontrol not only for single molecules at low temperatures in solids, but also for useful variants of the green fluorescent protein at room temperature [2]. This lecture describes the context of the events leading up to these advances as well as a portion of the subsequent developments both internationally and in my laboratory.

In the mid-1980s, I derived much early inspiration from amazing advances that were occurring around the world where single nanoscale quantum systems were detected and explored for both scientific and technological reasons. Some of these were (i) the spectroscopy of single electrons or ions confined in vacuum electromagnetic traps [3–5], (ii) scanning tunneling microscopy (STM) [6] and atomic force microscopy (AFM) [7], and (iii) the study of ion currents in single membrane-embedded ion channels [8]. But why had no one achieved optical detection and spectroscopy of a single small molecule deep inside a more complex condensed phase environment than in a vacuum, which would enable single-molecule spectroscopy (SMS)?

There was a problem. Years before, the great theoretical physicist and cofounder of quantum mechanics, Erwin Schrödinger stated [9]:

> ". . . we *never* experiment with just *one* electron or atom or (small) molecule. In thought-experiments we sometimes assume that we do; this invariably entails ridiculous consequences . . . In the first place it is fair to state that we are not *experimenting* with single particles, any more than we can raise *Ichthyosauria* in the zoo."

And he was not the only one who felt this way, even in the 1980s. Many scientists believed that, even though single photoelectrons might be detected from

photoionization of a single molecule in a vacuum, optically detecting a single molecule in a condensed phase sample was impossible. Thus the key aspect of the early part of this story is to explain how I got to the point to believe that it would be possible.

1.2 Low temperature spectroscopy of molecules in solids: Inhomogeneous broadening

In order to explain the initial SMS experiments in the late 1980s, it is necessary to briefly review some concepts from high resolution optical spectroscopy of molecular impurities in solids, a field of intense study in the decades surrounding 1970 driven by names such as E. V. Shpol'skii, R. Personov, K.K. Rebane, and others. (Exhaustive references cannot be included here, but for a comprehensive text covering many aspects, see [10].) Beginning at room temperature, let us consider the optical absorption spectrum of terrylene molecules dispersed at low concentration (say 10^{-6} mol/mol) in a solid transparent host of *p*-terphenyl (see Fig. 1). The figure shows the optical absorption expressed in optical density of a sample vs the wavelength λ of light used for probing, the kind of spectrum one can obtain from a commercial uv-vis spectrometer. A color scale shows the correspondence to the colors of visible light. Starting with long wavelengths on the right, there is no absorption, and as λ gets shorter (energy gets higher according to $E = \mathbf{h}f$ with **h** Planck's constant, f frequency), eventually the molecule absorbs light. The arrow shows the first electronic transition representing the promotion of an electron from the ground state (highest occupied molecular

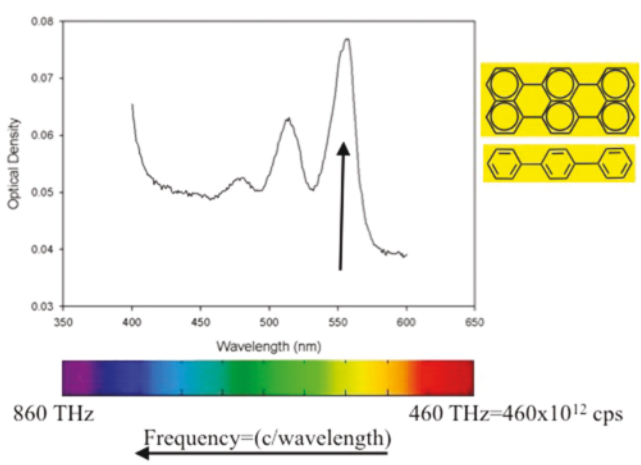

FIGURE 1. Spectrum (absorption vs. wavelength, or color) of terrylene molecules in a solid host of *p*-terphenyl at room T.

orbital) to the first excited state (lowest unoccupied molecular orbital). The shorter wavelength absorptions shown involve the creation of additional vibrations in the molecule. In addition, since f and λ are inversely related ($f = \mathbf{c}/\lambda$ with $\mathbf{c}$ the speed of light), if λ increases to the right, then frequency increases to the left. The frequencies at the edges of the plot are shown, in the range of hundreds of THz (10^{12} cycles per second).

Terrylene (and other similar aromatic hydrocarbons) is a relatively planar, rigid molecule which is held flat by the π orbitals of the molecule and the bonds that are denoted by the aromatic rings of the molecule. Because of this, the first electronic transition does not involve large distortions of the molecule, that is, this transition involves primarily the electronic degrees of freedom, also termed minimal Franck-Condon distortion. Now let's cool the sample to very low temperatures of a few K above absolute zero (liquid helium temperatures), and expand the horizontal scale by roughly 25 times. Spectroscopists often switch between wavelength and frequency displays, and Fig. 2 now shows frequency increasing to the right, in units of wavenumber or inverse cm; 1 cm^{-1} corresponds to roughly 30 GHz. Only a small piece of orange wavelengths are left. At such low temperatures, the vibrations of the molecule cannot be thermally excited, so the appearance of the first electronic transition is now extremely narrow. Moreover, the vibrations of the solid (phonons) are essentially nonexistent too, so they cannot contribute to broadening of the optical absorption, and the line becomes a "zero-phonon" line. In fact, in the *p*-terphenyl host crystal,

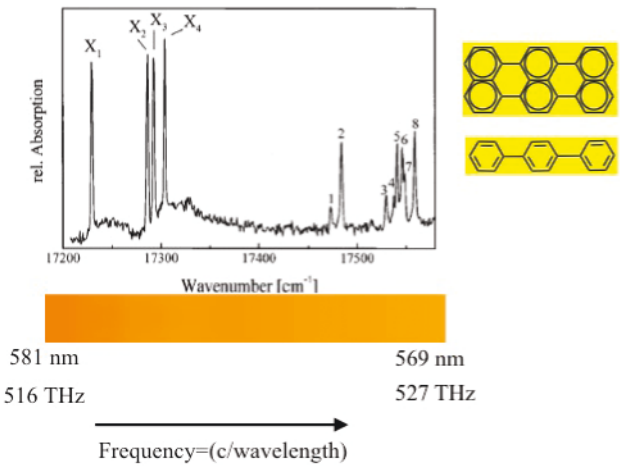

FIGURE 2. Spectrum (absorption vs. frequency/wavenumber, or color) of terrylene molecules in a solid host, *p*-terphenyl, at low T (~2K), from Ref. [10½].

there are four inequivalent locations for the terrylene molecules in the crystal, thus there are four "origins": X_1–X_4, because the structure of the host in these four different sites are quite different. The absorption lines have become narrow enough so that the different perturbations coming from the different local environments (think local pressure) are now observable.

In fact the spectrum in Fig. 2 does not tell the whole story, because the width of the absorption line for any one of the four sites is far narrower than shown. To fully resolve the absorption line in a way not limited by the apparatus, spectroscopists began to use narrowband dispersing devices such as double monochromators or ultimately single frequency continuous wave (cw) tunable lasers as light sources, but a further surprise was waiting. Figure 3(a) shows the situation for pentacene dopant molecules in *p*-terphenyl crystals at 1.8 K as reported by Orlowski and Zewail in 1979 [11]. One might expect that now the linewidth should be only about 10 MHz or so, the expected width for the molecular absorptions as limited only by the lifetime of the excited state. However, the absorption profile is much wider, about 0.7 cm^{-1} or about 21 GHz! This excess width was recognized as *inhomogeneous broadening* as schematized in Figure 3(b). The various molecules in the solid have intrinsically narrow widths (called the homogeneous width), but the overall absorption line profile represents the range of different center frequencies for the molecules arising from different local environments (illustrated in Figure 3(c)) which shift the absorption energies over a range. These perturbations arise from effects like local stresses and strains arising from crystal imperfections, or from other defects, or possibly from local electric fields, and so on, and a number of theoretical models were proposed for the mechanisms of inhomogeneous broadening [12].

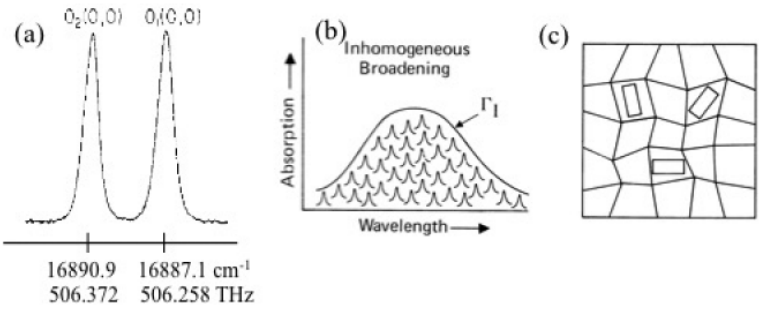

FIGURE 3. Inhomogeneous broadening in solids at low temperatures. (a) Pentacene in *p*-terphenyl absorption spectra taken from Ref. [11] (0.09 cm-1 resolution). (b) Schematic of the inhomogeneous broadening effect with width Γ_I. (c) Schematic of different local environments giving rise to inhomogeneous broadening.

1.3 The environment at IBM Research: Spectral hole-burning for optical storage

One goal of high-resolution spectroscopy was to measure the true homogeneous width of the zero-phonon, purely electronic transition of molecules in solids without the interference from inhomogeneous broadening. It is for this reason that much research in the 1970s and 1980s was devoted to methods like fluorescence line narrowing (FLN) [13, 14] and transient spectroscopies such as free induction decay, optical nutation, and photon echoes [15–17]. While these were all powerful methods with advantages and disadvantages, there was another method to assess the homogeneous width under certain circumstances, persistent spectral hole-burning, illustrated in Figure 4. This optical effect was discovered in the 1970s by two Russian groups: by Gorokhovskii et al. for H_2-phthaocyanine in a Shpol'skii matrix [18], and by Kharlamov et al. for perylene and 9-aminoacridine in glassy ethanol [19]. Persistent spectral hole-burning turned out to be a fairly common effect in the optical transitions of impurities in solids at low temperatures. Given an inhomogeneously broadened line (Figure 4 upper), irradiation with a narrowband laser only excites the subset of molecules resonant with the laser within a homogeneous width Γ_H. Spectral hole-burning

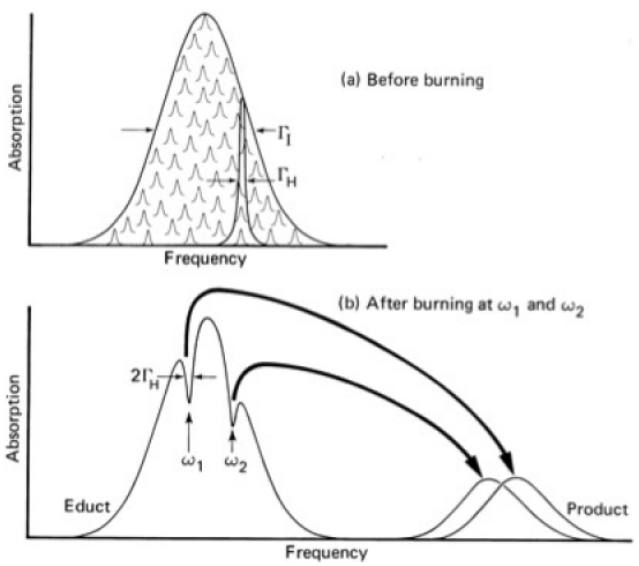

FIGURE 4. Illustration of persistent spectral hole-burning in inhomogeneous broadened lines of dopants in solids at low temperatures. (a) Before burning, the inhomogeneously broadened line has a "smooth" absorption profile. (b) When a narrowband laser irradiates selected frequencies in certain materials, spectral dips or "holes" can be generated.

occurs when light-driven physical or chemical changes are produced only in those molecules resonant with the light, driving these molecules to some other part of frequency or wavelength space. This leaves behind a dip or "spectral hole" in the overall absorption profile of width roughly 2 Γ_H. Importantly, it was realized by scientists at IBM Research that hole-burning may be used for optical recording of information in the optical frequency domain, hence the term "frequency domain optical storage" [20]. For more detail on spectral hole-burning see Ref. [21].

In 1981, I joined one of the great corporate research labs at the time, IBM Research, to work on materials and mechanisms for spectral hole-burning storage. This was a time where a novel idea with potential application could be studied in great detail in a corporate research center, from the fundamental scientific issues to the development of the required materials, to the potential engineering design of the system. Persistent spectral hole-burning was of interest because it would enable many bits of information to be stored in the same spot in the optical frequency domain simply by choosing to either write a hole or not write a hole in the inhomogeneously broadened line profile. Since for a number of systems the ratio Γ_I / Γ_H was on the order of 1000 or more at low temperatures, a huge increase in optical storage capacity was envisioned. Mechanisms for the process could be photochemical [22] where the light induces a photochemical change, or photophysical (nonphotochemical), where only the two-level systems of the nearby host need be changed [23, 24], and much effort centered on the generation of new materials systems. Unfortunately, in the end the need for low temperatures and the amazing compound growth rate of magnetic storage performance squeezed this idea out of practical application, although microwave signal processing applications [25] are still being explored using hole-burning effects.

1.4 Statistical fine structure in inhomogeneously broadened lines

Luckily, it was also important at IBM to examine the fundamental limits to new technologies for optical storage, and this was particularly interesting to me. In 1985, I worked with Marc Levenson on the shortcomings of one-photon (linear) hole-burning mechanisms [26]. As spectral holes are written at higher and higher speed, the actual depth of the hole will get smaller up until it has a fractional depth equal to the one-cycle quantum efficiency for spectral hole formation. In addition to shot noise due to Poisson number fluctuations of the probing light, we realized that a particularly interesting additional limitation on the signal-to-noise ratio of a spectral hole might result from the finite number of

molecules that contribute to the absorption profile near the hole. The question arose: Is there a static spectral roughness on the inhomogeneous line that results from *statistical number fluctuations or the discreteness of individual molecules*? This would define one ultimate limit on the smallest spectral hole that could be detected. The basic idea is illustrated from familiar probability considerations in Figure 5. Supposing that 50 balls are thrown randomly at 10 bins, it is quite unlikely that exactly 5 balls will land in each bin (Fig 5(a)). Rather, a much more likely outcome of a single experiment is shown in Figure 5(b): the numbers landing in each bin will have an *average* value of 5 over all bins, but the actual numbers will scatter above and below this value. This is the familiar number fluctuation effect, equivalent to the scaling of the standard error of the mean, where the rms size of the fluctuations about the mean will scale as $\sqrt{N}$, where N is the average number in each bin, or $\sqrt{5}$ in this case. The central limit theorem applies here since the molecules are assumed independent.

Now to see how this idea relates to high resolution spectroscopy of inhomogeneously broadened lines at low temperatures, we simply think of the horizontal axis as optical frequency (or wavelength), and imagine that Γ_I is extremely large so that the inhomogeneous line appears locally flat on the scale of the page. Each box is a bin of width Γ_H, the homogeneous width of an optical absorption line, and molecules pick frequencies when the sample is formed in a random way. Then the resulting spectrum should have a *spectral roughness* or *fine structure* scaling as $\sqrt{N}$, which arises from the discreteness of the individual molecules! This can also be seen in the simulation of Figure 5(c), where a (perfectly

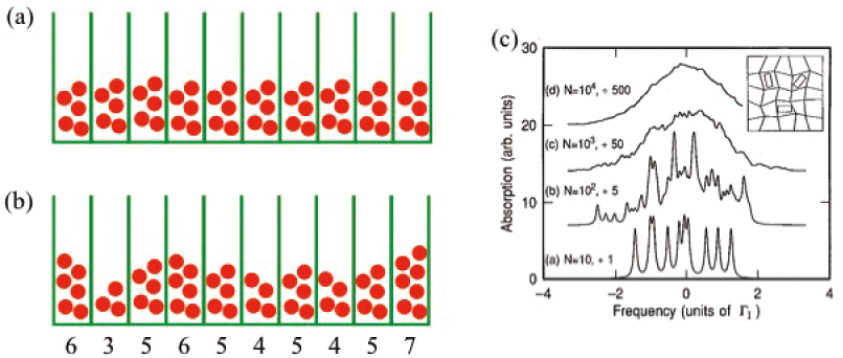

FIGURE 5. Illustration of number fluctuations for probability and for spectroscopy. (a) An unlikely way to randomly throw 50 balls at 10 bins. (b) A more likely case. (c) Simulation of an inhomogeneously broadened line in a sample for the case of uniform Gaussian probability of selecting absorption frequencies, with N being the total number simulated in this figure.

smooth) Gaussian shape was assumed for the probability of molecules to assume specific resonance frequencies. At very small numbers of total molecules, the variations in absorption are obvious, and at larger and larger concentrations, the effect appears to smooth out, as was likely the case in the early spectra of pentacene in *p*-terphenyl in Figure 3(a) [11]. (In addition, the spectral resolution was too low to see this effect in the early experiments.) It is critical to note that this effect is not "noise" in the usual sense of time-dependent interfering fluctuations, but rather a *static* variation in absorption *vs* wavelength or optical frequency. We named this effect "statistical fine structure" (SFS), and it is important to realize that the *relative* size of SFS gets smaller at high concentration as $\left(1/\sqrt{N_H}\right)$, while the absolute root-mean-square (rms) size of the fine structure *grows* as $\sqrt{N_H}$. Surprisingly, prior to the late 1980s, the observation of SFS had not been reported, so this was a first goal.

In 1987, my postdoc Tom Carter and I observed SFS for the first time [27, 28], using a powerful zero-background optical absorption technique, laser frequency-modulation (FM) spectroscopy [29, 30], explained below. The choice of sample was critical: We actually tried for many months to see the effect for perylene dopant molecules in a thin film of poly(vinyl chloride), but each time we scanned the spectrum and saw a hint of the structure, it changed for the next

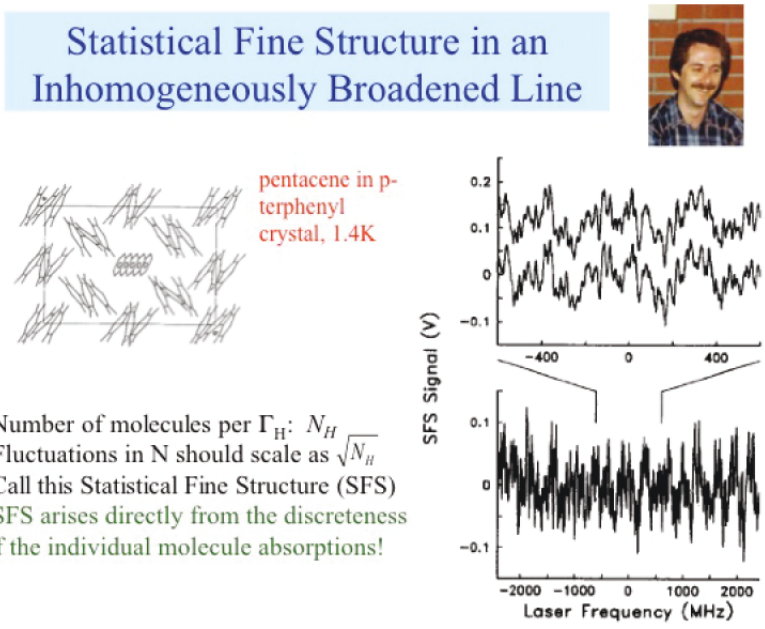

FIGURE 6. Observation of Statistical Fine Structure (SFS) (right) for pentacene in *p*-terphenyl (schematic structure) with Tom Carter (photo). Data after Ref. [28].

scan! This was due to photophysical hole-burning for this system caused by the probing laser. At one point, in frustration due to the need for a system with no hole-burning, I consulted Michael Fayer at Stanford, who suggested pentacene dopant molecules in a *p*-terphenyl crystal (Figure 6, left). Over the weekend, I simply melted some *p*-terphenyl laced with a tiny speck of pentacene on a hot plate between glass slides, put it in the cryostat, and we immediately saw the SFS signal! Figure 6, right, shows a small 5 GHz slice of the O_1 site inhomogeneous line centered roughly at 506 THz. SFS is the amazing spectral structure which repeats beautifully when the scan is repeated (upper panel). SFS is clearly unusual, in that its size depends not upon the total number of resonant molecules, but rather upon the square root of the number, and it arises directly from the discreteness of the individual molecules. (It turns out that hole-burning was not completely absent in this system, but only far less probable-with extended laser irradiation, spectral holes could be burned directly in the SFS.)

2. SINGLE-MOLECULE DETECTION, SPECTROSCOPY, AND IMAGING AT LOW TEMPERATURES

2.1 FMS and a scaling argument led the way to the first single-molecule detection and spectroscopy in condensed phases

The other crucial aspect of the SFS experiment was the ultrasensitive optical detection method used, laser FM spectroscopy (FMS) [29, 31]. FMS was invented by Gary C. Bjorklund at IBM in 1980, and he taught me this method to be able to use it for detection of spectral holes. As illustrated in Figure 7, a single-frequency tunable laser at frequency ω_C passes through an electro-optic phase modulator and acquires frequency modulation at an rf modulation frequency ω_M, usually on the order of 100 MHz. In the frequency domain, two sidebands appear as shown. These sidebands are out-of-phase, so that if they are not disturbed by the sample, a fast detector which naturally measures the envelope of the light wave produces no signal at ω_M. However, when a narrow spectral feature (narrow on the scale of ω_M) is present, the imbalance in the laser sidebands leads to amplitude modulation in the detected photocurrent at ω_M which is easily detected by rf lock-in techniques. In other words, the sample converts the FM beam into an AM beam when a narrow feature is present, and the whole experiment behaves roughly like FM radio at 506 THz (albeit at low modulation index). A key feature of FMS is that it senses only the deviations of the absorption from the average value, more precisely, the signal is proportional to $\alpha(\omega_C+\omega_M)-\alpha(\omega_C-\omega_M)$ with α the absorption coefficient. This is the

main reason why the detection of SFS could be easily accomplished with FMS. There was no need to make an heroic sample with ultralow concentration to see SFS, because the SFS signal measured by FMS is actually larger with higher concentrations of molecules!

Nevertheless, with the detection of SFS in hand, it now became possible for me to believe that single-molecule detection would be possible. This key point can be understood by a simple scaling argument: When SFS due to ~1000 molecules is detectable (roughly the case in Fig. 6), that means that the measured FMS signal (rms amplitude) is the same size as ~32 molecules (i.e., $(1000)^{1/2}$). But this means that in terms of improving the signal-to-noise ratio (SNR) of the FMS apparatus, it was only necessary to work 32 times harder to observe a single molecule, not 1000 times harder! This realization, combined with two additional facts: (i) FM absorption spectroscopy was insensitive to any Rayleigh or Raman scattering background from imperfect samples, and (ii) FMS allows quantum-limited detection sensitivity, led me and my postdoc Lothar Kador (Fig. 8) to push FM spectroscopy to the single-molecule limit. It is also true that the particularly low quantum efficiency for spectral hole-burning made pentacene in *p*-terphenyl an excellent first choice for single-molecule detection.

The first SMS experiments in 1989 utilized either of two powerful double-modulation FMS absorption techniques, laser FMS with Stark electric field secondary modulation (FM-Stark) or FMS with ultrasonic strain secondary modulation (FM-US) [1, 32]. Secondary modulation was required in order to remove the effects of residual amplitude modulation produced by the imperfect phase

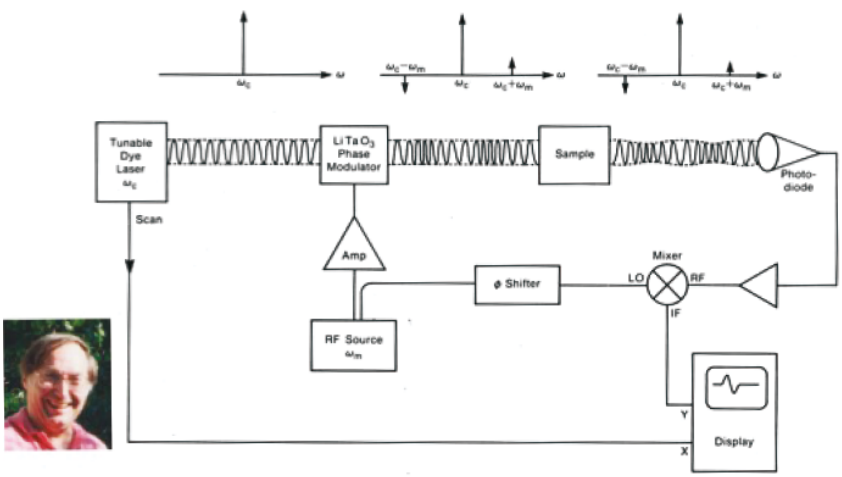

FIGURE 7. Laser frequency-modulation spectroscopy for detection of weak absorption and dispersion signals. Photo: Gary C. Bjorklund. From Ref. [33].

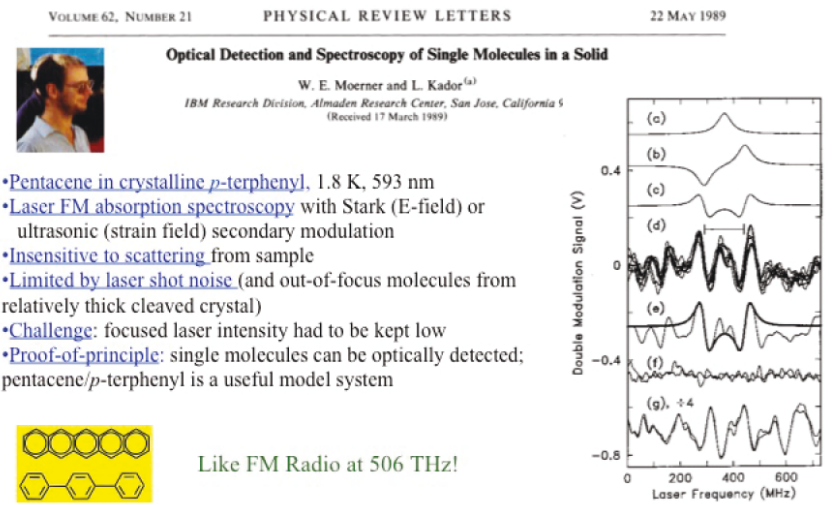

FIGURE 8. First optical detection and absorption spectroscopy of single molecules in condensed matter. (a–c) Buildup of expected lineshape for FM-Stark spectroscopy. (d) Multiple scans showing a single molecule at 592.423 nm. (e) Averaged scans compared to lineshape. (f) Far into the wings of the line, no molecule. (g) Closer to the center of the inhomogeneous line; SFS. Photo: Lothar Kador. From Ref. [1].

modulator [33]. Figure 8 (specifically, trace d) shows examples of the optical absorption spectrum from a single molecule of pentacene in *p*-terphenyl using the FM-Stark method, where the laser center frequency was simply tuned into the wings of the inhomogeneously broadened line in order to select the single-molecule concentration range without growing a new sample with reduced doping.

Although this early observation and similar data from the FM-US method served to stimulate much further work, there was one important limitation to the general use of FM methods for SMS. As was shown in the early papers on FMS [29, 31], extremely weak absorption features as small as 10^{-7} in relative size can be detected in a 1 s averaging time, but only if large laser powers on the order of several mW can be delivered to the detector to force the photon shot noise to dominate the detector Johnson noise. However, in SMS, the laser beam must be focused to a small spot to maximize the optical transition probability, thus the power in the laser beam must be maintained below the value which would cause saturation broadening of the single-molecule lineshape, which is hard to avoid for such a narrow line at low temperatures. As a result, the data of Fig. 8 had to be acquired with powers below 100 μW at the detector, which is one reason why the SNR was only on the order of 5. (The other reason was the

use of relatively thick cleaved samples, which produced a population of weaker out-of-focus molecules in the probed volume. This problem was subsequently easily overcome.) In later experiments by Lothar [34], frequency modulation of the absorption line itself (rather than the laser) was produced by an oscillating (Stark) electric field alone, and this method has also been used to detect the absorption from a single molecule at liquid helium temperatures. While successful, these transmission methods are limited by the quantum shot noise of the laser beam, which is relatively large at the low laser intensity required to prevent saturation.

2.2 Crucial milestone: detection of single-molecule absorption by fluorescence

The optical absorption experiments on pentacene in *p*-terphenyl indeed showed that this material has sufficiently inefficient spectral hole-burning to make it a useful model system for single-molecule studies. In 1990, Michel Orrit and Jacky Bernard demonstrated that sensing the optical absorption by detection of the emitted fluorescence produces superior signal-to-noise if the emission is collected efficiently and the scattering sources are minimized [35]. Due to its relative simplicity, subsequent experiments have almost exclusively used this method, which is also called "fluorescence excitation spectroscopy." It is an application of the gas-phase method of laser-induced fluorescence pioneered by R. N. Zare in 1968 [36] to solids. In fluorescence excitation, a tunable narrowband single-frequency laser is scanned over the absorption profile of the single molecule, and the presence of absorption is detected by measuring the fluorescence emitted (Figure 9) to long wavelengths, away from the laser wavelength itself. The method is often background-limited, and it requires the growth of ultrathin crystal clear sublimed flakes to reduce the scattering signals that could arise from the *p*-terphenyl crystal, but it does not suffer from the difficult tradeoff between SNR and optical broadening of FMS. This was a major advance for single-molecule spectroscopy, and if there were a fourth recipient for the Nobel Prize, Michel Orrit should have received it.

With the ability to detect single molecules in crystals and polymers, in the early 1990s many investigators all over the world jumped into the field in order to take advantage of the extremely narrow optical absorption lines and the removal of ensemble averaging, two of the largest motivations for the study of single molecules. Investigations were sometimes directed at specific observations of particular effects like the Stark effect [37], two-level system dynamics [38], or polarization effects [39] to name a few. At other times experiments were performed simply to observe, because surprises would be expected when a new

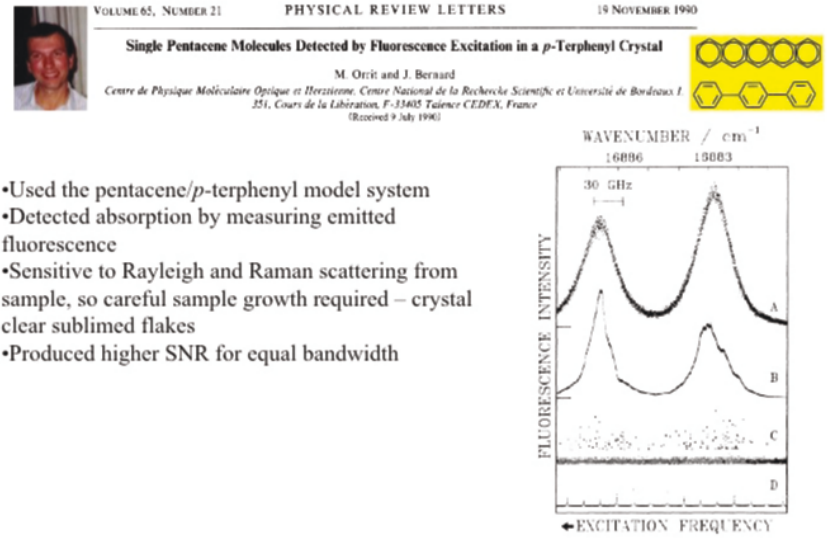

FIGURE 9. Single-molecule detection and absorption spectroscopy by recording the emitted fluorescence. A, B, the inhomogeneous line, C, at very low concentration, the dots represent the increases in emission when single molecules come into resonance with the tunable laser. Photo: Michel Orrit. From Ref. [35].

regime is first explored. The great body of work done is too large to review here, and the reader is referred to selected texts [21, 40] and selected review articles [41–47] for more information. My talented group of postdocs and collaborators completed a wide array of experiments, including measurements of the lifetime-limited width, temperature-dependent dephasing, and optical saturation effects [48, 49], photon antibunching correlations [50], vibrational spectroscopy [51–53], magnetic resonance of a single molecular spin [54], and near-field spectroscopy [55]. Some experiments have particular relevance for super-resolution microscopy and will be discussed next.

2.3 Single-molecule spectroscopy and imaging

With the single-molecule sensitivity that became available in the early 1990s, a more detailed picture of inhomogeneous broadening appeared. Figure 10(a) shows a scan over the inhomogeneously broadened optical absorption profile for pentacene in *p*-terphenyl; compare Fig. 3(a). While molecules overlap near the center of the line at 592.321 nm (0 GHz), in the wings of the line, single, isolated Lorentzian profiles are observed as each molecule comes into resonance with the tunable laser. The situation is very much like tuning your AM radio to

find a station while far away from big cities: you tune and tune, mostly hearing static, until you come into resonance with a station, then the signal rises above the static. It is obvious that with a lower-concentration sample, single molecules at the center of the inhomogeneous line could also be studied, and the line profile is only Gaussian near the center—there are large non-Gaussian tails quite far away from the center. These beautiful spectra provided much of the basis for the early experiments. For example, at low pumping intensity, the lifetime-limited homogeneous linewidth of 7.8+/–0.2 MHz was directly observed (Figure 10(b)) [56]. This linewidth is the minimum value allowed by the lifetime of the S_1 excited state of 24 ns, in excellent agreement with previous photon echo measurements on large ensembles [15, 57]. Such narrow single-molecule absorption lines are wonderful for the spectroscopist: many detailed studies of the local environment can be performed, because narrow lines are much more sensitive to local perturbations than are broad spectral features.

Going beyond spectral studies alone, a hybrid image of a single molecule was obtained by Pat Ambrose in my lab by acquiring spectra as a function of the position of the laser focal spot in the sample [48]. Spatial scanning was accomplished in a manner similar to confocal microscopy by scanning the incident laser beam focal spot across the sample in one spatial dimension. Figure 10(c) shows such a three-dimensional "pseudo-image" of single molecules of

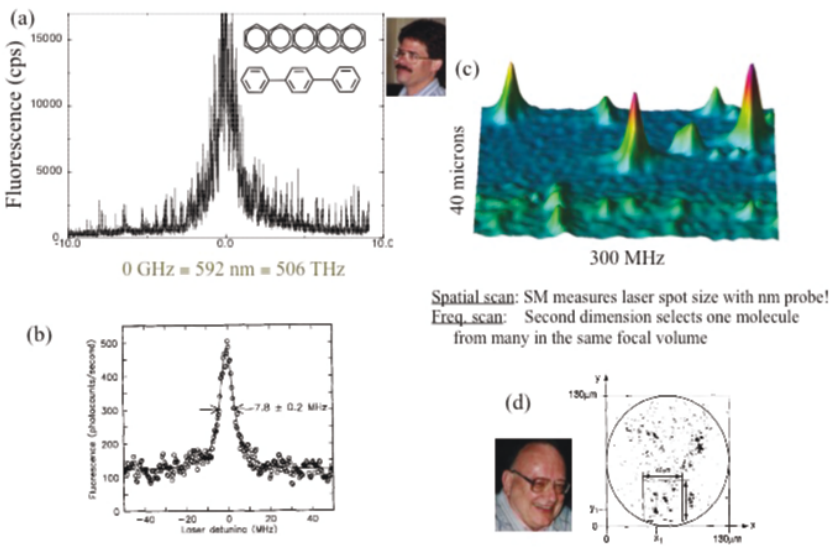

FIGURE 10. (a,b) Single-molecule spectroscopy and (c,d,) imaging. Photos: W. Pat Ambrose (upper), Urs P. Wild (lower). From Refs. (a) [49], (b) [56], (c) [48], (d) [58].

pentacene in *p*-terphenyl. The *z*-axis of the image is the (red-shifted) emission signal, the horizontal axis is the laser frequency detuning (300 MHz range), and the axis going into the page is one transverse spatial dimension produced by scanning the laser focal spot (40 μm range). In the frequency domain, the spectral features are fully resolved because the laser linewidth of ~3 MHz is smaller than the molecular linewidth. However, considering this image along the spatial dimension, the single molecule is actually serving as a highly localized nanoprobe of the laser beam diameter itself (here ~5 μm, due to the poor quality of the focus produced by the lens in liquid helium) [48]. The molecule can be regarded as a nanometer-sized probe of the focal spot, which is roughly equivalent to a measurement of the point-spread-function (PSF) of the imaging system. This is the first example of a spatial image of a single molecule PSF, discussed in more detail below. Soon thereafter, the Wild laboratory in Switzerland [58] obtained two-dimensional images of the shape of a single-molecule spot as shown in Figure 10(d) in reverse contrast.

2.4 Surprises—spectral diffusion and optical control

During the early SMS studies on pentacene in *p*-terphenyl, an unexpected phenomenon appeared: resonance frequency shifts of individual pentacene molecules in a crystal at 1.5 K [48, 56], mentioned briefly earlier [35]. We called this effect "spectral diffusion" due to its close relationship to similar spectral-shifting behavior long postulated for optical transitions of impurities in amorphous systems [59]. Here, spectral diffusion means changes in the center (resonance) frequency of a single molecule due to configurational changes in the nearby host which affect the frequency of the electronic transition via guest-host coupling. For example, Fig. 11(a) shows a sequence of fluorescence excitation spectra of a single pentacene molecule in *p*-terphenyl taken as fast as allowed by the available SNR, every 3 s. The spectral shifting or hopping of this molecule from one resonance frequency to another from scan to scan is clearly evident. Now if the laser frequency is held fixed near the molecular absorption, then the molecule appears to blink on and off as it jumps into and out of resonance (Fig. 11(b), at two power levels). Due to the lack of power dependence on the rate, these spontaneous processes suggested that there are two-level systems available in the host matrix which can undergo thermally induced transitions even at these low temperatures. One possible source for the tunneling states in this crystalline system could be discrete torsional librations of the central phenyl ring of the nearby *p*-terphenyl molecules about the molecular axis. The *p*-terphenyl molecules in a domain wall between two twins or near lattice defects may have

lowered barriers to such central-ring tunneling motions. A theoretical study of the spectral diffusion trajectories by Jim Skinner and co-workers [60–62] postulated specific defects that can produce this behavior, attesting to the power of SMS in probing details of the local nanoenvironment and the importance of theoretical insight to further understanding. Spectral shifts of single-molecule lineshapes were observed not only for certain crystalline hosts, but also for essentially all polymers studied, and even for polycrystalline Shpol'skii matrices [63]. This is a dramatic example of the heterogeneity that was uncovered by the single-molecule studies.

With my postdoc Thomas Basché, light-driven shifts in absorption frequency were also observed for perylene dopant molecules in poly(ethylene), in which the rate of the process clearly increased with increases in laser intensity [64, 65], Figure 11(c). This photoswitching effect may be called "spectral hole-burning" by analogy with the earlier hole-burning literature [21]; however, since only one molecule is in resonance with the laser, the absorption line simply disappears. Subtraces (a), (b), and (c) show three successive scans of one perylene molecule. After trace (c) the laser was tuned into resonance with the molecule, and at this higher irradiation fluence, eventually the fluorescence signal dropped, that is, the molecule apparently switched off. Trace (d) was then

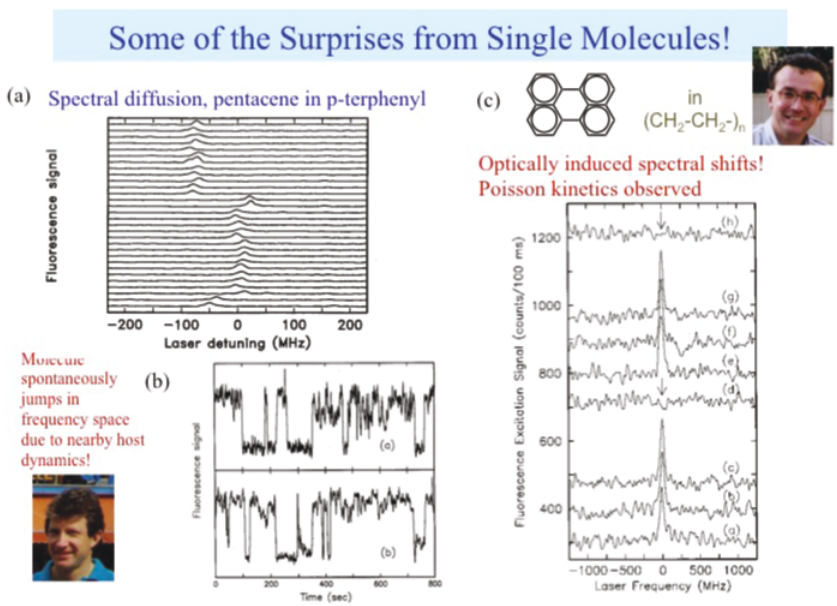

FIGURE 11. (a,b) Spectral diffusion and (c) light-induced spectral shifts. From Refs. [48], [56], [64], respectively. Photos: (L) Jim Skinner, (R) Thomas Basché.

acquired, which showed that the resonance frequency of the molecule apparently shifted by more than +/−1.25 GHz as a result of the light-induced change in the nearby environment. Surprisingly, this effect was reversible for a good fraction of the molecules: a further scan some minutes later (trace (e)) showed that the molecule returned to the original absorption frequency! After trace (g) the molecule was photoswitched again and the whole sequence could be repeated many times, enabling us to measure the Poisson kinetics of this process from the waiting time before a spectral shift [65].

Several single-molecule systems showed light-induced shifting behavior at low temperature, for example, terrylene in poly(ethylene) [66], and terrylene in a Shpol'skii matrix [67]. Optical modification of single-molecule spectra not only provided a unique window into the photophysics and low-temperature dynamics of the amorphous state, this effect presaged another area of current interest at room temperature: photoswitching of single molecules between emissive and dark forms is a powerful tool currently being used to achieve super-resolution imaging (*vide infra*).

3. INTERLUDE—WHY STUDY SINGLE MOLECULES?

Before continuing with room-temperature studies, it is useful to recount some of the key motivations and advantages of this approach. Single-molecule spectroscopy (SMS) allows *exactly one* molecule hidden deep within a crystal, polymer, liquid, or cell to be observed via optical excitation of the molecule of interest. This represents detection and spectroscopy at the ultimate sensitivity level of ~1.66×10^{-24} moles of the molecule of interest (1.66 yoctomole), or a quantity of moles equal to the inverse of Avogadro's number. Detection of the single molecule must be done in the presence of trillions of solvent or host molecules. To achieve this, a light beam (typically a laser) is used to pump an electronic transition of the one molecule resonant with the optical wavelength, and it is the interaction of this optical radiation with the molecule that allows the single molecule to be detected. Successful experiments must meet the requirements of (a) guaranteeing that only one molecule is in resonance in the volume probed by the laser, and (b) providing a signal-to-noise ratio (SNR) for the single-molecule signal that is greater than unity for a reasonable averaging time.

Why are single-molecule studies now regarded as a critical part of modern physical chemistry, chemical physics, and biophysics (Figure 12)? By removing ensemble averaging, it is now possible to directly measure distributions of behavior to explore hidden heterogeneity. This heterogeneity might be static,

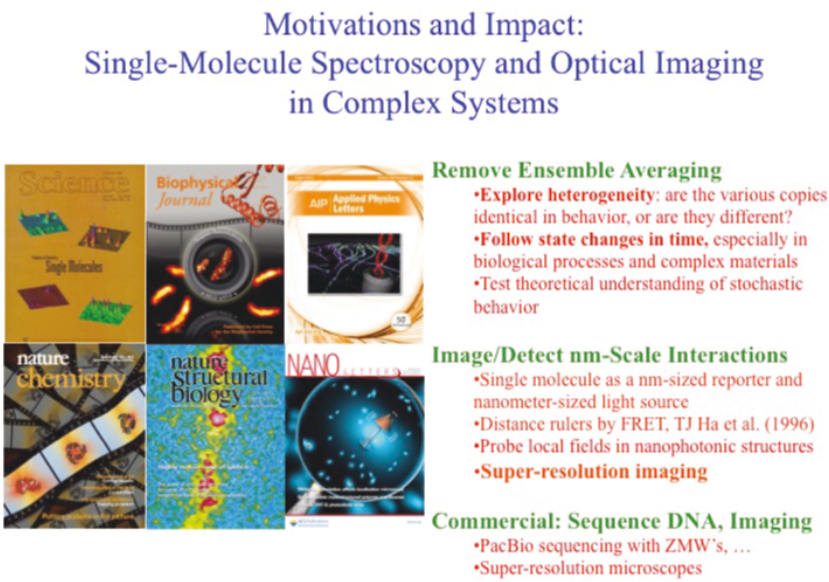

FIGURE 12. Motivations and impact, with selected journal covers from the Moerner lab.

arising from differences in the way in which the single molecule interacts with the nearby (complex) environment. Or it might occur in the time domain, arising from the internal states of one molecule and the transitions among them, and SMS then allows measurement of hidden kinetic pathways and the detection of rare short-lived intermediates. Because typical single-molecule labels behave like tiny light sources roughly 1–2 nm in size and can report on their immediate local environment, single-molecule studies provide a new window into nanoscale interactions with intrinsic access to time-dependent changes. Förster resonant energy transfer (FRET) with single molecules allows detection of conformational changes on the scale of ~ 5 nm [68]. Because the single molecule interacts with light primarily via the local electromagnetic field and the molecular transition dipole moment, enhanced local fields in metallic nanophotonic structures can be probed [69, 70]. The use of a single molecule as a nm-sized light source is one key property used in super-resolution microscopy, described in more detail below after the room temperature SMS studies are summarized. Finally, single molecules have found commercial application, both in DNA sequencing and in microscopy beyond the diffraction limit. The impact of being able to optically study the smallest individual component in a complex system is deep and broad.

4. ROOM TEMPERATURE STUDIES OF SINGLE MOLECULES

Soon after the first low-temperature experiments, studies began of single molecules at room temperature. A selection of key milestones is described in Table 1 to the best of my knowledge.

Early steps arose out of the development of "fluorescence correlation spectroscopy" (FCS) [72, 73], a large body of work which has been extensively reviewed in [88–90]. The method depends upon the fluctuations in emission from a tightly focused spot in solution arising from passage of molecules diffusing through a laser beam. Autocorrelation analysis of the fluorescence provides a window into a variety of dynamical effects on time scales less than the transit time on the order of 1–10 ms. The contrast ratio of the autocorrelation degrades at high concentrations but improves at low, and in 1990 correlation functions were recorded from concentrations so low that much less than one molecule was in the probe volume [77]. The passages of many single molecules must be

TABLE 1. Room temperature milestones of single-molecule detection and imaging.

Solution: Correlation functions	Fluorescence Correlation Spectroscopy (FCS): Magde, Elson, Webb 1972 [71–74]; Ehrenberg, Rigler 1974 [75]; Aragón, Pecora 1976 [76]; . . .
	Autocorrelation detected from 1 fluorophore or less in the volume: Rigler, Widengren 1990 [77]
Solution: Single bursts	Multichromophore emitter bursts (phycoerythrin): Peck, Stryer, Glaser, Mathies 1989 [78]
	Single bursts of fluorescence from 1 fluorophore: Shera, Seitzinger, Davis, Keller, Soper 1990 [79]; Nie, Zare 1994 [80]; . . .
Solution and surface	Single antibody with multiple (~80–100) labels: Hirschfeld 1976 [81]
Near-Field NSOM, SNOM Imaging	Imaging a single fluorophore: Betzig, Chicester 1993 [82]; Ambrose, Goodwin, Martin, Keller 1994 [83]; Xie, Dunn 1994 [84]
Confocal imaging	Macklin, Trautman, Harris, Brus 1996 [85]; . . .
Widefield, single fluorophore imaging	*In vitro*, single myosin on actin: Funatsu, Harada, Tokunaga, Saito, Yanagida 1995 [86]
	Cell membrane, single-lipid tracking with super-localization: Schmidt, Schütz, Baumgartner, Gruber, Schindler 1996 [87]

averaged; it is impossible to study only one molecule at a time for a long period with FCS.

Also in 1990, the Keller lab at Los Alamos used a carefully designed hydrodynamic flow to reduce the volume producing interfering background signals and directly detected the individual fluorescence bursts as individual single rhodamine 6G molecules passed through the focus [79]. This was a key step in reducing backgrounds, but there is great value in being able to watch the same single molecule for extended periods, measuring signal strength, lifetime, polarization, fluctuations, and so on, all as a function of time and with the express purpose of directly detecting any heterogeneity from molecule to molecule. Hirschfeld reported detection of a single antibody with 80–100 fluorophores in a short report much earlier in 1976 [81], but photobleaching and the optical apparatus available at the time limited further work.

A key milestone in single-molecule imaging at room temperature occurred in 1993, when near-field scanning optical microscopy (NSOM) was used to lower the pumped volume and hence potential interfering backgrounds [82–84]. It was subsequently demonstrated that with careful sample preparation and optimal detection, single molecules could be imaged with far field techniques such as confocal microscopy [85], wide-field epifluorescence, and total internal reflection fluorescence microscopies [86]. Of particular importance for cell biology applications, in 1996 Schmidt et al. explored the diffusion of single labeled lipids on a cell surface [87]. The explosion of methods allowing single-molecule detection and imaging has led to a wealth of exciting research in this area, with advances far too numerous to review comprehensively [91–93], and two sets of Nobel conference proceedings have appeared [94, 95].

4.1 Basics of single-molecule detection and imaging at room temperature

For concreteness, it is useful at this point to briefly summarize the basic detection strategy used in modern single-molecule studies at room temperature. Figure 13 illustrates some of the key ideas for the case of cellular imaging, but the method works for any type of sample as long as the experiment is designed to strictly reduce background and maximize the detected emission from the single molecule. Various textbooks and reviews may be consulted for additional detail [96–99]. Typically, organic fluorophore labels (such as TMR: tetramethyl rhodamine, cyanine dyes like Cy3, Alexa dyes, etc.) or fluorescent protein labels are attached to the biomolecule of interest, which may be a protein, lipid, sugar, or an oligonucleotide. The pumping light typically excites the energy levels of the fluorophore as sketched at the upper right, most often an allowed singlet-singlet

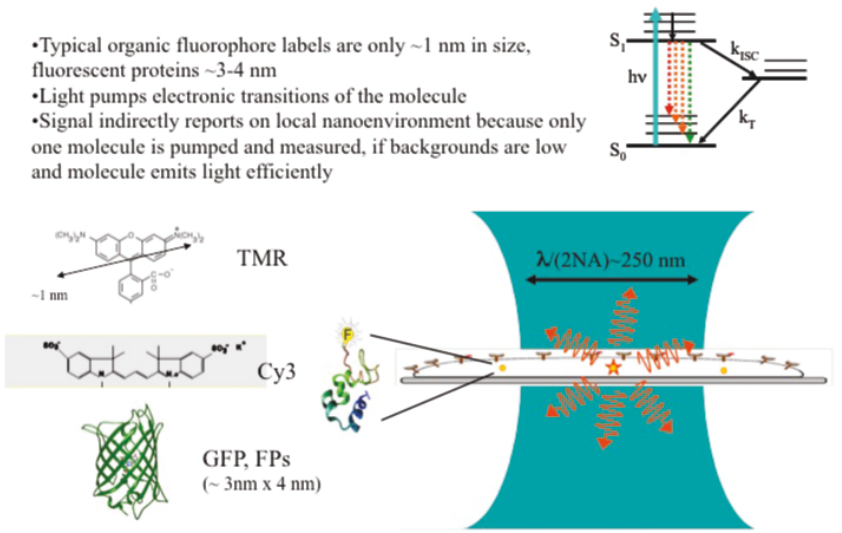

FIGURE 13. Overview of single-molecule detection and imaging at room temperature. From Ref. [139].

transition. Vibrational relaxation can occur before fluorescence is emitted red-shifted to longer wavelengths, a useful feature that helps in the detection process—typically long-pass filters are used to block any scattered pump light. Intersystem crossing can occur to triplet states, but usually fluorophores are chosen to minimize the time in dark states, except when blinking is required. No matter what microscope is used, we can without loss of generality think of one diffraction-limited pumping volume, which irradiates the sample on a typically transparent substrate. Of note is the well-known diffraction limit here: with far-field optics, the focal spot cannot be made smaller than $\lambda/(2\,\mathrm{NA})$ with NA the numerical aperture of the microscope. In the visible this limit corresponds to about 250 nm, and the contrast between the size of the focal spot and the size of the fluorescence labels (a few nm) is dramatic. Nevertheless, if the concentration of labeled molecules is kept low, only one molecule is pumped, and the emitted fluorescence reports on that labeled molecule in comparison to the spectral tunability which selects different molecules at low temperatures, here brute force dilution keeps the molecules separate.

Even without super-resolution methods which resolve dense emitters beyond the diffraction limit (discussed below), many single-molecule studies have been and will continue to be performed where individual separated molecules are imaged and observed over time. Simply following the motion of the single molecules gives information about the behavior of the molecules. Figure 14

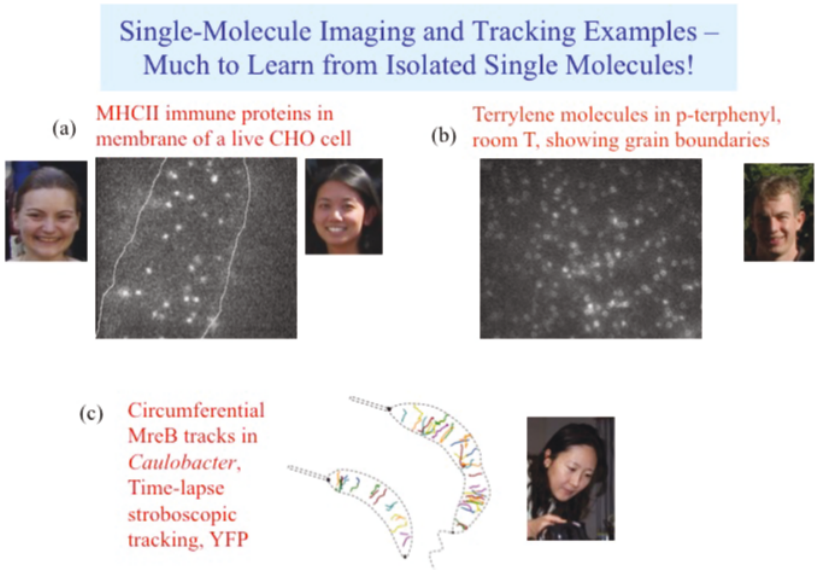

FIGURE 14. Selected single-molecule imaging and tracking studies at room temperature. From Refs. (a) [158]; (b) [104]; (c) [108]. Photos (L-R): Marija Vrljic, Stefanie Nishimura, Christopher (Kit) Werley, So Yeon Kim.

illustrates several selected examples of experiments of this type in the Moerner laboratory from the early 2000s. Figure 14(a) shows an image of single MHCII (major histocompatibility complexes of type II) proteins anchored in the plasma membrane of a CHO (Chinese hamster ovary) cell. A high affinity antigenic peptide was labeled with a single fluorophore to light up the MHCII molecules, and a real-time fluorescence video of the motion of these molecules shows the amazing dance of MHCII's which occurs on the surface of live cells. The diffusive properties of the motion and the influence of cholesterol were studied by my students in collaboration with Harden McConnell [100–103].

To give a materials science example, Figure 14(b) shows a fluorescence image of single molecules of terrylene in a spin-coated crystal of *p*-terphenyl [104]. Close inspection of the image shows that some molecules are small rings, while others are unstructured spots. The rings can be understood as the expected *z*-oriented dipoles [105], which are located in well-ordered crystalline regions of the sample. But more information can be found by watching the images as a function of time, see the Supporting Information of Ref. [104]. Surprisingly, even in this room temperature crystal, the unstructured spots move around, with highly biased diffusion along roughly horizontal and vertical lines in the sample. These single molecules are likely moving in the cracks of the sample;

thus the single-molecule motions can be used to visualize the defects in the crystal.

As a final example of the power of single-molecule tracking, for more than a decade now, the bright and red-shifted emission from single molecules of enhanced yellow fluorescent protein (EYFP) have led to its use as a label for fusions to interacellular proteins in the Moerner lab in collaboration with the laboratory of Lucy Shapiro and Harley McAdams [105½]. The primary organism of interest has been *Caulobacter crescentus*, because cells of this organism display asymmetric division in the cell cycle: one daughter cell has a flagellum while the other has a stalk with a sticky end. This means that the cells have a genetic program that causes different groups of proteins to appear in the two different daughter cells, and understanding this process would contribute to the general problem of understanding development [106, 107]. The basic effect arises from spatial patterning of regulatory proteins, which leads to many interesting questions: how do the proteins actually produce patterns, how do these patterns lead to different phenotypes in the daughter cells, and so on. Figure 13(c) shows what we observed for single fusions of EYFP to the cytoskeletal protein MreB in living cells [108]. One population of MreB molecules were diffusing as expected in the cytoplasm. However, on a long time scale, time-lapse imaging showed single molecules undergoing clear directed motion along linear tracks in a circumferential pattern around the edge of the cell. The figure shows tracks for single molecules in different cells, and while this observation was initially thought to involve treadmilling of filaments, this behavior is likely associated with MreB molecules interacting with the cell wall synthesis machinery [109].

4.2 Toward super-resolution: Key idea #1 is superlocalization of single-molecule emitters

We are now in a good position to address super-resolution microscopy with single molecules directly. As is well-known, biological fluorescence microscopy benefits from a variety of labeling techniques which light up different structures in cells, but the price often paid for using visible light is the relatively poor spatial resolution compared to x-ray or electron microscopy. Here "resolution" is used in the precise sense to mean the ability to distinguish two objects that are close together. The basic problem briefly mentioned above is that in conventional far-field microscopes, Abbe's fundamental diffraction limit (DL) [110] restricts the resolution to a value of roughly the optical wavelength λ divided by two times the numerical aperture (NA) of the imaging system, $\lambda/(2\ \mathrm{NA})$. Since the largest values of NA for state-of-the-art, highly corrected immersion

microscope objectives are in the range of about 1.3–1.6, the spatial resolution of optical imaging has been limited to about ~200–250 nm for visible light of ~500 nm wavelength.

In fact, the light from single fluorescent molecular labels about 1–2 nm in size provides a way around this problem, that is, a way to provide "super-resolution," or resolution far better than the diffraction limit. (Stimulated emission depletion microscopy (STED [111]) and structured illumination microscopy (SIM [112]) are other methods that surpass the DL but do not require single molecules and are discussed by Stefan Hell and Eric Betzig elsewhere.) How can single molecules help? The sketch in Figure 13 illustrated the typical imaging problem at room temperature: the single molecule is far smaller than the focused laser spot, yet, if only one molecule is pumped, information related to one individual molecule and its local "nanoenvironment" can be extracted by detecting the photons from that molecule alone [45]. In terms of spatial resolution, however, when the image is formed, the observed "peak" from the single nanoscale source of light maps out the diffraction-limited point-spread function (PSF) of the microscope, because the molecule is a nanoscale light absorber, far smaller than the size of the PSF. (Rigorously, the single emitting molecule is not strictly a point source, but rather a dipole emitter [113], but this subtlety is not important for this discussion.) If many emitters are decorating a structure, the PSFs overlap to form a blurry image that is fundamentally "out-of-focus."

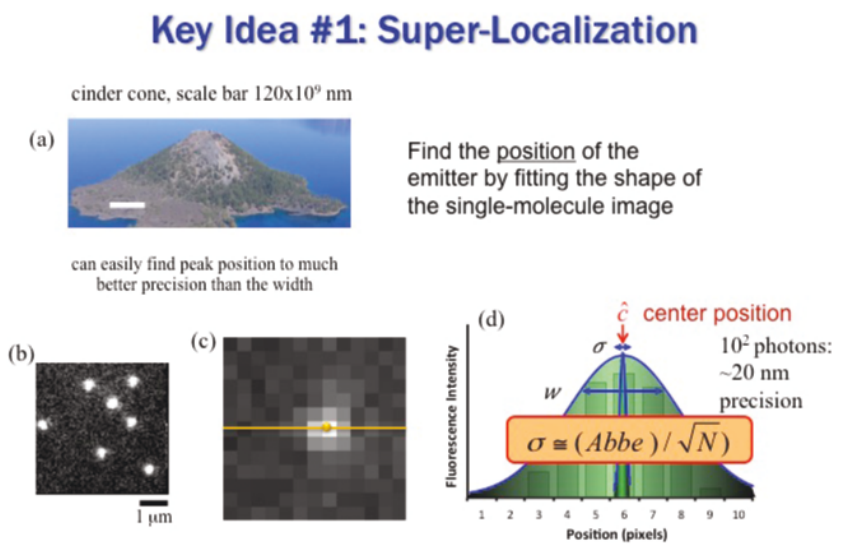

FIGURE 15. The central concepts behind super-localization of single-molecule emitters.

This problem was solved in a direct way by Betzig in 2006 [114], by simply preventing all the molecules from emitting at the same time and performing sequential imaging (see Section 4.4 below). For pedagogical simplicity, I will describe the basic ideas in their simplest form to underscore that the problem can be solved in a general way. One simply must follow two key steps: First, one must be able to acquire the image of a single molecule and localize its position with precision much better than the width of the PSF, a process that may be termed "super-localization." The second step, active control of the emitting concentration, will then be described in Section 4.4.

Figure 15 illustrates the basic concepts of super-localization of single molecules. To state an analogy, anyone can hike up to the top of the cinder cone in the center of Crater Lake, Oregon (Fig, 15(a)), and read out the GPS coordinates of the position of the mountain. This idea is effectively applied to single-molecule emitters: simply by measuring the shape of the PSF, the position of its center can be determined much more accurately than the PSF width. For example, with a wide-field image of single molecules in Fig, 15(b), the diffraction-limited spots are evident. It is essential to spread out each detected spot on multiple pixels of the camera as shown in Fig. 15(c). Then, illustrated by a 1D cross-section in Fig. 15(d), the various pixels detect different numbers of photons according to the shape of the PSF. Formally the PSF is an Airy function, but it may be approximated by a Gaussian function for simplicity, especially in the presence of background. The photon numbers detected in the various pixels provide samples of the function, which may be fit mathematically. While the width of this fit is still diffraction-limited with width $\hat{w}$, the estimate of the center position $\hat{c}$ follows a much narrower error distribution with standard deviation σ, which is generally called the "localization precision." The precision with which a single molecule can be located by digitizing the PSF depends fundamentally upon the Poisson process of photon detection, so the most important variable is the total number of photons detected above background N, with a weaker dependence on the size of the detector pixels and background [115–117]. The leading dependence of σ is just the Abbe limit divided by the square root of the number of photons detected. This functional form makes sense, since each detected photon is an estimate of the molecular position, so for N measurements, the precision improves as expected. Super-localization means that if 100 photons are detected, then the precision can approach 20 nm, and so on. Clearly, then, emitters with the largest numbers of emitted photons before photobleaching are preferable.

Fitting images to find the center position of an object is not a new concept in science, having been applied to experimental data analysis for some time [121]. In fact, Heisenberg knew in 1930 that the resolution improvement improved by

TABLE 2. Early applications of super-localization of single objects in biological imaging.

Find centroid of large fluorescent object	LDL (Low-Density Lipoprotein particles with many labels) on cell surface: Barak, Webb 1982 [118]
	Tracking kinesin motor-driven 190 nm bead with few nanometer precision: Gelles, Schnapp, Sheetz 1988 [119]
Find position of single fluorophore	Cell membrane, ***single-lipid tracking to 30 nm precision***:
	Schmidt, Schütz, Baumgartner, Gruber, Schindler 1996 [87]
	Single virus particle on HeLa Cell to 40 nm precision:
	Seisenberger, . . . Bräuchle 2001 [120]

one over the square root of the number of photons detected [122]. For concreteness, this discussion will be restricted to biological imaging, and Table 2 lists some of the early applications to my knowledge. The early cases applied the idea to objects larger than the diffraction limit such as a LDL particle [118] or a fluorescent bead [119], and then the localization determined is just the position of the centroid of the large object. More interesting for the present discussion is the case when a single fluorophore is emitting, and this type of super-localization was first used for tracking single lipids to 30 nm precision by Schmidt et al. [87]. A subsequent cellular example addressed single virus particle tracking in the process of cellular entry [120]. As another example of an *in vitro* study, digitization of the PSF for single Cy3 fluorescently-labeled myosin molecules was used to extract position information down to a few nm by Yildiz et al. [123], and a new acronym was proposed (FIONA, for Fluorescence Imaging with One Nanometer Accuracy). The knowledge that the same molecule is emitting all the detected photons means that an N-photon correlation is being measured; as long as the photons are independent, the same analysis applies. When more complex photon states can be used in the future, the situation will change.

4.3 Surprises for single fluorescent protein molecules: blinking and photocontrol

Another exciting trend in the 1990s was the advent of genetically expressed green fluorescent proteins, an area of great importance for molecular and cellular biology which ultimately won the Nobel Prize in Chemistry for Osamu Shimomura, Martin Chalfie, and Roger Y. Tsien in 2008 [124]. Indeed, having just left IBM in 1995 for the University of California, San Diego, I was able to

broaden my interests in single molecules to include biology and room temperature studies. My postdoc, Robert Dickson, and I first worked to achieve partial immobilization of single small organic molecules in aqueous environments using the water-filled pores of poly(acrylamide) gels [125]. Then in 1996, noting the fast-moving events with fluorescent proteins, I had the opportunity to obtain samples of a new yellow fluorescent protein mutant (YFP) from Andy Cubitt in Roger Tsien's laboratory. As opposed to GFP, which has two absorption bands and undergoes excited state proton transfer from the shorter wavelength band to the longer wavelength form before emission [126], YFP was designed to stabilize the long-wavelength form, and it could be pumped with one of our Ar^+ ion laser lines at 488 nm. Robert Dickson and I then proceeded to see if we could detect and image single copies of YFP at room temperature. Using total internal reflection fluorescence (TIRF) microscopy, Rob was able to record the first images of single fluorescent proteins in a gel in 1997 [2] as shown in Figure 16(a).

These early experiments also yielded the first example of a room temperature single-molecule optical switch [2] and the first details of the photophysical character of GFP variants on the single-copy level. The experiments actually utilized two red-shifted GFP variants (S65G/S72A/T203Y denoted "T203Y" and S65G/S72A/T203F denoted "T203F") which differ only by the presence of a hydroxyl

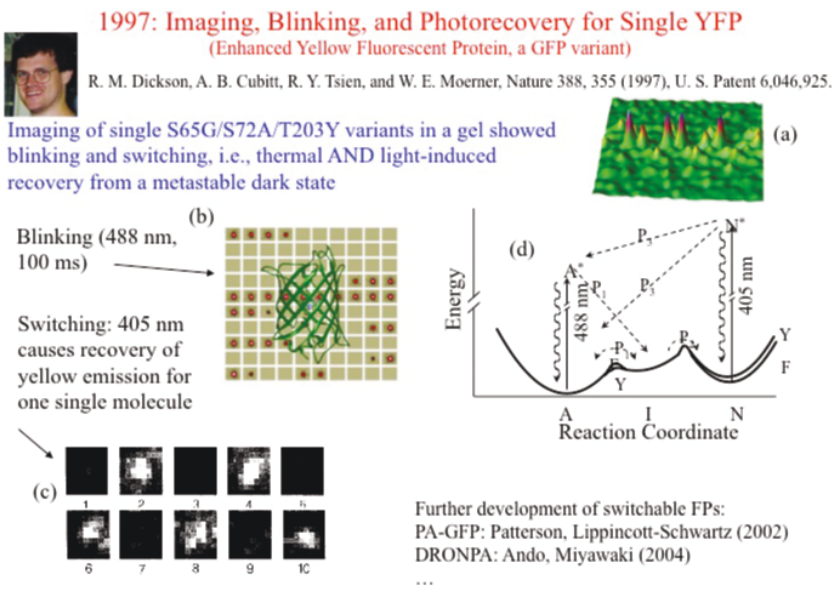

FIGURE 16. Imaging (b), blinking (b), and light-induced photorecovery or switching (c,d) for single YFP. Photo: Rob Dickson. From Ref. [2].

group near the chromophore, both of which are quite similar to the widely used enhanced yellow fluorescent protein EYFP (S65G/V68L/S72A/T203Y). In particular, a fascinating and unexpected blinking behavior appeared, discernable only on the single-molecule level (see the background of Fig.16(b) for a series of fluorescence images of one molecule for example). This blinking behavior likely results from transformations between at least two states of the chromophore (A and I, Fig. 16d), only one of which (A) is capable of being excited by the 488 nm pumping laser and producing fluorescence. Additionally, a much longer-lived dark state *N* was observed upon extended irradiation. Thermally stable in the dark for many minutes, this long-lived dark state was not actually permanently photobleached, rather we found that a little bit of light from a lamp at 405 nm would regenerate the original fluorescent state as shown in the sequence of images in Fig. 16(c). This means that the protein can be used as an emitting label until it enters the long-lived dark state, and then it can be photo-restored back to the emissive form with the 405 nm light, a reversal of the apparent photobleaching. When Rob and I observed this blinking and light-induced restoration for single copies of YFP, the thought at the time was the possibility that the photoswitching could be used for optical storage, and a patent was awarded.

The ability to optically control the emissive states of fluorescent proteins quickly expanded, as other researchers around the world engineered many new photoswitchable fluorescent proteins (such as Kaede [127], PA-GFP [128], EosFP [129], and DRONPA [130]). These interesting molecules with colorful names were to soon play a critical role in the final key idea leading to super-resolution microscopy.

4.4 Key idea #2: Active control of the emitting concentration, and sequential imaging

Super-localization works fine when molecules are spatially separated, but what can be done when they are overlapping in the same volume? How can the spatial resolution of such blurry images be improved? It is worth remembering that the low temperature high-resolution spectroscopy described in Section 2 above provided a potential clue to this problem: Even within the same diffraction-limited spot, many different molecules could easily be separately selected simply by tuning the laser—the resonance frequency was a control variable that effectively turned the molecules on and off so that they would not interfere. But we were simply not thinking of spatial resolution in the early 1990s, because we had plenty of *spectral* resolution! At the same time, in the mid-1990s, progress was being made toward general methods of solving the spatial resolution problem, as summarized in Table 3.

TABLE 3. Steps toward super-resolution with single-molecule emitters. For acronyms, see [139].

Key proposal	Use some additional control variable to separate DL spots in spatial dimension—spectral tunability suggested: E. Betzig 1995 [131]
Low T	Spectral tunability used to achieve 3D super-resolution:
	40 nm lateral, 100 nm axial for several single molecules
	A. van Oijen, J. Köhler, J. Schmidt, M. Müller, G. J. Brakenhoff 1998 [132, 133]
Room T	Multicolor imaging of single fluorescent probes: T.D. Lacoste, X. Michalet, F. Pinaud, D.S. Chemla, A.P. Alivisatos, S. Weiss 2000 [133½]
	Distinguish two dyes by fluorescence lifetime:
	M. Heilemann, D.P. Herten, R. Heintzmann, C. Cremer, C. Müller, P. Tinnefeld, K.D. Weston, J. Wolfrum, M. Sauer 2002 [134]
	Use photobleaching of overlapping fluors:
	SHRImP: M. P. Gordon, T. Ha, P.R. Selvin 2004 [135]
	NALMS: X. Qu, D. Wu, L. Mets, N.F. Scherer 2004 [136]
	Two differently colored probes:
	SHREC: L.S. Churchman, Z. Oekten, R.S. Rock, J.F. Dawson, J.F. Spudich 2005 [137]
	Blinking of semiconductor quantum dots:
	K.A. Lidke, B. Rieger, T.M. Jovin, R. Heintzmann 2005 [138]

In 1995, after spending years developing near-field optical imaging at Bell Labs, Eric Betzig wrote a seminal paper noting that a control variable that distinguishes molecules along another dimension could be used for super-resolution microscopy, and he suggested the use of many molecules with different colors, as in the low temperature studies [131]. Subsequently, in 1998 Antoine van Oijen *et al.* experimentally demonstrated this idea directly: they used spectral tunability at low temperatures to spatially resolve a set of single molecules in three dimensions, with 40 nm lateral and 100 nm axial resolution, far below the optical diffraction limit [132, 133]. Of course, biological applications could only become widespread if the problem could be solved at room temperature, and researchers continued to try out new ideas to resolve closely spaced molecules. Multicolor imaging of differently colored beads or quantum dots was used to super-resolve a handful of closely-spaced emitters [133½]. Another strategy

involved using the fluorescence lifetime differences between probes to separate them [134], demonstrated for two dyes spaced 30 nm apart. Other strategies used naturally occurring photobleaching—eventually all molecules will bleach except one. Adding further to the exploding menagerie of acronyms, this basic idea was demonstrated by Gordon et al. for Cy3 labels on DNA [135] (SHRImP, for Single-molecule High-Resolution Imaging with Photobleaching) and by Qu et al. using Cy3-labeled PNA probes on DNA [136] (NALMS, for NAnometer Localized Multiple Single-molecule fluorescence microscopy). By separately imaging two fluorophores (Cy3 and Cy5) attached to two different calmodulin molecules that bind to the "legs" of the same single molecule of myosin V, distance measurements accurate to ~ 10 nm were achieved, and a another acronym was generated [137, 140] (SHREC, for Single-molecule High-REsolution Colocalization of fluorescent probes). Lidke et al. showed that a certain degree of super-resolution beyond the diffraction limit could also be achieved with the blinking of fluorescent semiconductor quantum dots [138].

The stage was now set for several concepts to be put together to yield a general method for super-resolution microscopy with single molecules, and Key Idea #2 is illustrated in Figure 17. A structure has been labeled with many fluorescent labels as shown on the left, and when all are allowed to emit simultaneously, the blurry image results because the many PSFs overlap. The key idea is simply to *not* allow all the molecules to emit at the same time! Let us suppose that there is some mechanism which allows the emitters to be on part of

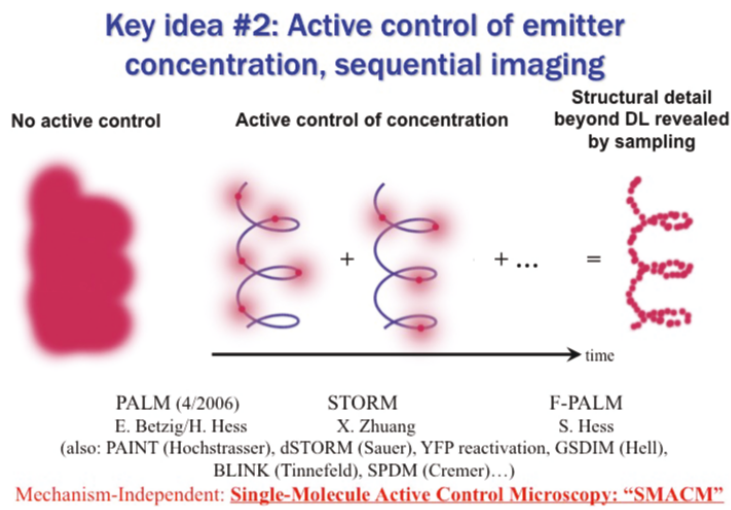

FIGURE 17. Active control of emitting concentration leads to super-resolution microscopy. After Ref. [155].

the time and emitting photons, and off, or dark, another part of the time. The experimenter uses this mechanism to *actively control the concentration of emitting molecules to a very low level* such that the PSFs do not overlap. Then using super-localization in one acquired image of the molecules, the positions of those are determined and recorded. Then these molecules are turned off or photobleached, and another subset is turned on, super-localized, etc. In the end, after a number of sequential imaging cycles, many locations on the structure have been sampled using the tiny single-molecule "beacons," and the underlying image is reconstructed in a pointillist fashion to show the detail previously hidden beyond the diffraction limit as shown on the right. Effectively, then, the overlapping molecular positions are determined by time-domain multiplexing.

I first heard about this idea from Eric Betzig and his primary collaborator, Harald Hess, in April 2006 at the Frontiers in Live Cell Imaging Conference at the NIH main campus in Bethesda, Maryland. They used the PA-GFP fluorescent proteins of George Patterson and Jennifer Lippincott-Schwartz [128] and other photoswitchable fluorescent proteins as an active control mechanism, terming the method PALM (for PhotoActivated Localization Microscopy) [114]. Light-induced photoactivation of GFP mutant fusions is used to randomly turn on only a few single molecules at a time in fixed cell sections or fixed cells. In their *tour de force* experiment, individual PSFs were recorded in detail to find their positions to ~ 20 nm, then were photobleached so that others could be turned on, and so on until many thousands of PSF positions were determined, and a super-resolution reconstruction was produced.

Very quickly after the NIH meeting, a flood of researchers demonstrated super-resolution imaging with single molecules using additional active control mechanisms and additional acronyms. The laboratory of Xiaowei Zhuang utilized controlled photoswitching of small molecule fluorophores for super-resolution demonstrations [141] (STORM, for STochastic Optical Reconstruction Microscopy). Their original method used a Cy3-Cy5 emitter pair in close proximity that shows a novel property: restoration of Cy5's photobleached emission can be achieved by brief pumping of the Cy3 molecule. In this way, the emission from a single Cy5 on DNA or an antibody is turned on by pumping Cy3 and off by photobleaching, again and again, in order to measure its position accurately multiple times. After many such determinations, the localization accuracy can approach ~20 nm precision, and labeled antibodies (labeled with >1 Cy3, <<1 Cy5) were used to localize RecA proteins bound to DNA. Samuel Hess et al. published an approach similar to Betzig's with an acronym termed F-PALM (Fluorescence PhotoActivation Localization Microscopy) [142], which also utilized a photoactivatable GFP with PSF localization to obtain superresolution.

Also in 2006, an alternative approach was reported by the laboratory of Robin Hochstrasser based on accumulated binding of diffusible probes, which are quenched in solution yet de-quench in close proximity of the surface of the object to be imaged [143] (termed PAINT, for Points Accumulation for Imaging in Nanoscale Topography). The method relies upon the photophysical behavior of certain molecules that light up when bound or constrained, and they demonstrated the idea with the twisted intermolecular charge transfer (TICT) state of Nile Red [144]. PAINT has advantages that the object to be imaged need not be labeled and that many individual fluorophores are used for the imaging, thus relaxing the requirement on the total number of photons detected from each single molecule.

Other active control mechanisms quickly appeared such as dSTORM [145] (direct STORM), GSDIM (Ground-State Depletion with Intermittent Return) [146], blinking as in BLINK-microscopy [147], SPDM (Spectral Precision Determination Microscopy) [148], and the list goes on. In 2008, Julie Biteen in my laboratory used the EYFP photorecovery mechanism described above to perform super-resolution imaging in bacteria [149], but since we did not create a new acronym for this, the work did not receive as much attention. Therefore, to jokingly add a new acronym to the field that is mechanism-independent, my lab informally uses the acronym SMACM, which stands for Single-Molecule Active Control Microscopy. In any case, the key underlying idea is very general, and PALM led the way. There are photochemical methods for single-fluorophore turn-on [150] and even enzymatic methods for turn-on which may be controlled by the concentration of substrate and the enzymatic rate [151]. The experimenter must choose actively use some method to control the emitting concentration. Of course, the imaging is still time-sequential, thus this approach is best for quasi-static structures or fixed cells, but significant progress has been made in increasing the imaging speed [152]. Selected reviews may be consulted for additional detail of modern challenges and progress [153–161].

4.5 Super-resolution microscopy applications and developments from the Moerner Lab

Since the early 2000's, my laboratory in the Stanford Chemistry Department has been in a fruitful collaboration with the microbiology and developmental biology laboratory of Lucy Shapiro to use advanced single-molecule imaging to explore regulatory protein localization patterns in a particularly interesting bacterium, *Caulobacter crescentus*. Since bacteria are very small, only a couple of microns long and submicron in diameter, the size of the entire organism is near the optical diffraction limit and super-resolution microscopy can be used

to great advantage. Thus, as mentioned in the last section, in 2007 we began single-molecule super-resolution imaging in bacteria, and took advantage of the photoinduced recovery and/or blinking of single EYFP we discovered in 1997 [2] as an active-control mechanism. Figure 18 illustrates how the raw data actually appear: Fig. 18(a) shows a white light transmission image of a field of cells, and Fig, 18(b) shows a single fluorescence frame after initial bleachdown. From many 10–50 ms frames such as these, super-localization is performed to extract single-molecule localizations, and super-resolution reconstructions can be generated.

Figure 19 illustrates some of the super-resolution images from three of our *Caulobacter* studies in recent years. The upper row shows what would be observed with diffraction-limited conventional fluorescence imaging, and the lower row shows SMACM super-resolution images of the same cells. In each column, a different target protein has been fused to EYFP. Column 1 shows imaging results from my postdoc at the time, Julie Biteen, on the MreB cytoskeletal protein which appears to form a quasi-helical structure [149]. (Later work noted that the helical shape is likely an artifact of the fluorescent protein construct that was used [162]. Super-resolution imaging naturally provides higher resolution that allows such effects to be observed, so additional care must now be taken to guard against labeling perturbation and to develop improved labels.) Column 2 shows ParA protein results generated by a collaboration between Jerod Ptacin from Lucy's lab and my postdoc, Steven Lee [163]. Involved in the process of chromosome segregation, ParA localized in a narrow linear structure running along the axis of the cell, which recedes during the translocation of the chromosomal origin from the old pole to the new pole. Finally, column

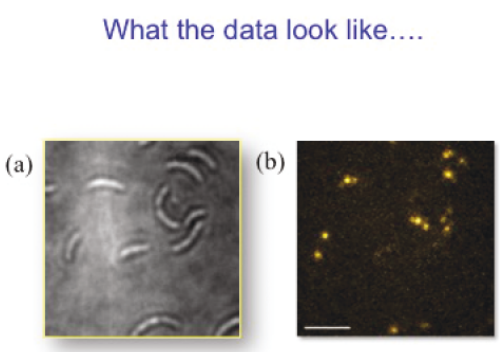

FIGURE 18. Raw data showing blinking of single EYFP fusions to a target protein in *Caulobacter* bacteria. (a) White light transmission image. (b) Single 10 ms frame of fluorescence image, 5 mm scale bar.

3 shows fixed-cell data for the nucleoid binding protein HU2, from work by Steven Lee and graduate student Mike Thompson [164]. Because HU2 binds nonspecifically to many locations on the chromosome, the localizations here provide useful information about the DNA distribution inside the cell which could be analyzed with spatial point statistics. Overall, these images show how important super-resolution imaging is in providing detail that could not be observed before, and super-resolution imaging is widely used for bacteria at present [165–167].

Of course, super-resolution imaging in eukaryotic cells is also a major area of current interest. In Figure 20, I include one example from my lab utilizing a novel method of achieving active control, which might be called target-specific PAINT, enabled by a collaboration with the synthetic chemistry laboratory of Justin Du Bois at Stanford [168]. Alison Ondrus, a postdoc in the Du Bois lab, was able to synthesize the potent neurotoxin molecule shown in Figure 20, saxitoxin (STX), with a covalently attached fluorescent label such as Cy5. Given this fluorescent ligand which binds to and blocks voltage-gated sodium (Na_V) channels, it was then possible for my graduate student, Hsiao-lu Lee, and a visiting scholar, Shigeki Iwanaga, to grow PC12 cells on a coverslip surface, induce them to differentiate into neural-like cells, and then simply provide the STX-Cy5 to the solution above the cells. The ligands in solution are not easily imaged due to their fast motion. Diffusion brings the STX-Cy5 to the cell surface

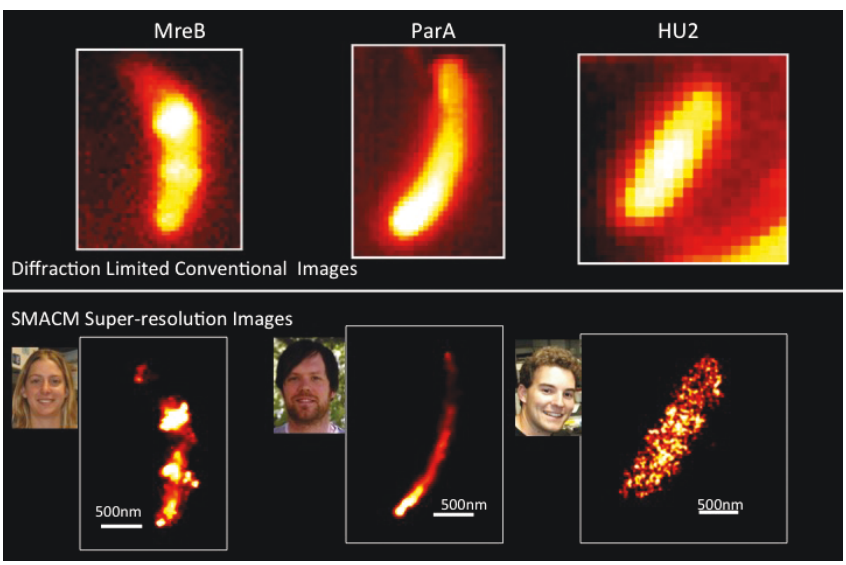

FIGURE 19. Super-resolution imaging of three different proteins in Caulobacter: MreB [149], ParA [163], HU2 [164]. Photos L-R: Julie Biteen, Steven Lee, Mike Thompson.

where the molecule binds to Na_V channels and provides a bright fluorescent spot for super-localization. The label then photobleaches and dissociates from the cell, allowing new ligands to bind. By recording a fluorescent movie, many single-molecule localizations could be continuously recorded and grouped to form a super-resolution reconstruction of the locations of the channels on the cell membrane. Figure 20 shows data recorded from axonal-like projections, where the panels on the right compare diffraction-limited and super-resolution reconstructions. By grouping all localizations within a 6.25 s interval, the sequence of images on the left shows how the cell changes over time, with various sub-diffraction neuritic extensions growing and retracting. It was also possible to record time-dependent images on a time scale of 500 ms by sliding boxcar averaging (see SI of Ref. [168].) Thus, with this method, a reasonable degree of time-dependent behavior can be observed, well beyond the diffraction limit.

Another recent application of PALM/SMACM to eukaryotic cells involved imaging of Huntingtin (Htt) protein aggregate structures in cells. The Htt protein leads to the neurodegenerative Huntington's disease when the poly(glutamine) repeat sequence is expanded. Super-resolution images of the aggregate structures were imaged in vitro by my graduate student Whitney Duim [169, 170]. In a collaboration with the laboratory of Judith Frydman at Stanford, my postdoc Steffen Sahl and graduate student Lucien Weiss grew neuronal model PC12m cells transfected with the mutant form of the Htt protein exon 1 fused to EYFP and imaged the fluorescence from fixed and live cells at various time points

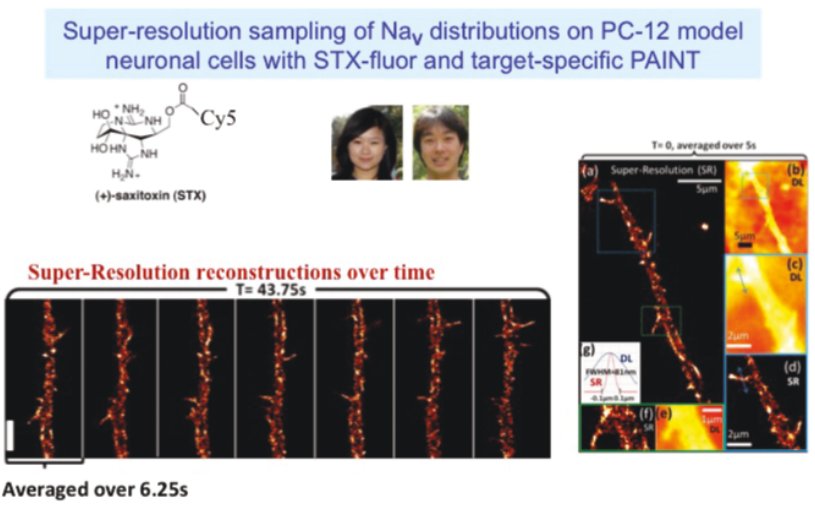

FIGURE 20. Example of super-resolution cellular imaging using a fluorescent saxitoxin ligand binding to ion channels on the cell surface. Bar in left sequence: 5 microns. From Ref. [168]. Photos: Hsiao-lu Lee, Shigeki Iwanaga.

post-transfection [171]. Critical to success of these experiments was targeted photobleaching of the extremely bright inclusion body (IB) before single-molecule imaging of the blinking EYFP. In this way, it was possible to observe tiny aggregate species in the cell body as shown in Figure 21(a), with reversed-contrast super-resolution reconstructions showing that these are small fibrillary structures. In axonal-like projections from the cells (Figure 21(b)), various small aggregate species are also observed with super-resolution detail. It is not fully known at the present time whether or not these small aggregate species are themselves toxic or the product of cellular processing to remove them, but being able to image and quantify such structures is an important start toward understanding the mechanism of the disease, and this method is being applied to other neurodegenerative disorders.

To end this very brief summary of super-resolution imaging with single molecules, I want to mention a couple of the outstanding challenges and current directions of development, using the illustrations in Figure 22. One area is the need for better fluorophores, specifically molecules with the ability to be turned on (and off) at will, with more emitted photons than are available from fluorescent proteins, for example. Small organic molecules generally offer ten times more total emitted photons than fluorescent proteins and could be less perturbative, so combining such molecules with a photochemical or photophysical mechanism for turn-on would be preferable. (Of course, it is also necessary

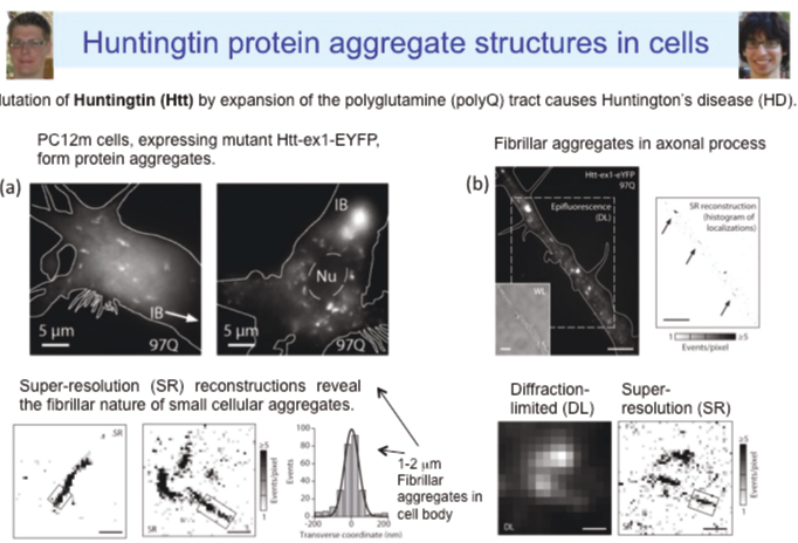

FIGURE 21. Super-resolution imaging of Htt fibrillary aggregates in cells. (a) Cell body, with 550 nm scale bar in the lower images. (b) Axonal processes. Scale bar 5 microns in upper images, 500 nm lower. Photos: Steffen Sahl, Lucien Weiss. From Ref. [171].

to target such molecules to appropriate biomolecules, and much effort is going on in this area, too.) The left side of Figure 22 shows a photoswitchable rhodamine spirolactam which has been modified by Prabin Rai in the laboratory of my synthetic collaborator, Robert Twieg at Kent State University, to undergo photoinduced turn-on by opening of the lactam ring with blue rather than ultraviolet light [172]. Using an N-hydroxysuccinimide derivative, my graduate student Marissa Lee covalently attached these molecules to the surface of live *Caulobacter* cells and then recorded super-resolution images of the cell surface. The images at the bottom show that this method produces excellent reconstructions with many localizations, and the sub-diffraction-sized bacterial stalks of varying lengths are easily observed and quantified.

Another area of intense current interest is the extension of super-resolution microscopy beyond two spatial transverse dimensions to three dimensions, *x*, *y*, and *z*. While some researchers have pursued astigmatic imaging [173], multiplane imaging [174, 175], or other approaches, my laboratory has concentrated on advanced methods of pupil-plane optical Fourier processing [176] to encode the *z*-position of single molecules in the shape of the PSF itself. Our first step in this area was in collaboration with Rafael Piestun of the University of Colorado to demonstrate that the double-helix point spread function (DH-PSF) can be used for single-molecule microscopy [177]. The right side of Figure 22, upper panel, shows that the DH-PSF operation converts the usual single spot from a

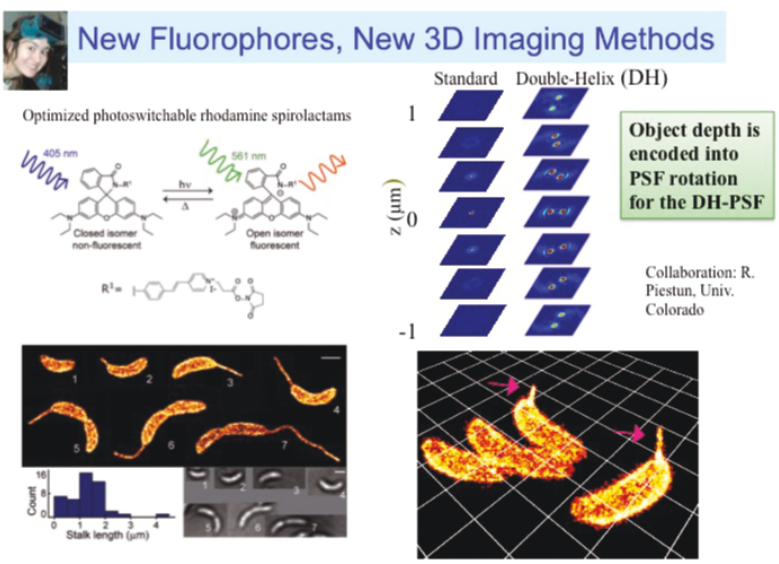

FIGURE 22. New photoswitchable fluorophores applied to bacterial imaging (left) and 3D imaging based on the DH-PSF (right). Photo: Marissa Lee. From Ref. [172].

single molecule into two spots that revolve around one another depending upon the *z*-position of the molecule in the sample. The angle of the line between the two spots encodes the *z*-position simultaneously for all molecules in the frame over a 2 micron depth of field. This approach has superior Fisher information and thus better localization precision than that of other approaches [178], and we have used the DH-PSF in two colors to co-image two different fluorescent protein fusions in *Caulobacter* [179] [159]. The lower half of Figure 22 shows the application of the DH-PSF method to 3D surface imaging of *Caulobacter* labeled by the rhodamine spirolactam [172]. Much remains to be done, as new point-spread function designs continue to appear [180–182], with the continuing goal to extract the maximum information from each tiny single-molecule emitter in the most efficient fashion.

5. CONCLUDING REMARKS AND ACKNOWLEDGEMENTS

In this contribution, the early steps leading to the first single-molecule detection and spectroscopy [27][1] were described. The low temperature imaging experiments in the early 1990s yielded many novel physical effects, such as spectral diffusion and light-activated switching which have reappeared in the later room temperature studies in different, but related forms. At room temperature, the surprising single-molecule blinking and photoswitching for single GFP variant molecules provided a pathway to the active control that was needed for PALM super-resolution microscopy and its relatives. Today, super-resolution microscopy is a powerful application of single molecules that has broad impact across many fields of science (Figure 23), and new and amazing discoveries continue, such as the observation of actin bands in axons [183]. All of this has occurred due not only to my efforts, but also due in major part to the clever and insightful research performed by many researchers around the world too numerous to mention here. Beyond super-resolution microscopy, just observing single molecules and their behaviors continues to lead to tantalizing scientific advances, whether this is simply tracking single-molecule motions [184], or inferring biomolecular interactions and conformations with FRET [185, 186] or extracting photodynamics from trapped single molecules [187] [188], or determining enzymatic mechanisms [189]. The future of single-molecule spectroscopy and super-resolution imaging is very bright.

I have been extremely fortunate throughout the entire period of my research career to have had the privilege of working with a team of brilliant and exceptional students and postdoctoral researchers. The Moerner Lab alumni are listed in Figure 24, and I warmly thank all of them for their hard work and insights. I am also extremely grateful to my current students and postdocs, pictured near

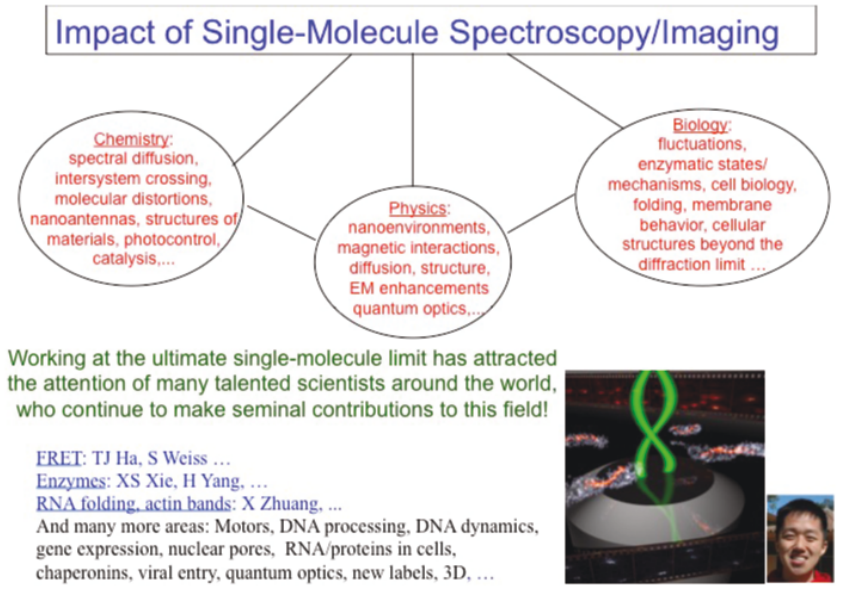

FIGURE 23. Impact of single-molecule spectroscopy and imaging, with selected examples. Multicolor 3D image of intracelleular proteins and cell surface courtesy Matthew Lew (pictured); see Ref. [179].

the Rodin Sculpture Garden on Halloween in Figure 25, along with our "No Ensemble Averaging" logo from Sam Lord. These talented scientists are continuing to push the field of single-molecule spectroscopy, trapping, imaging, and super-resolution into the future. The figure explains why we like to refer to one molecule as a "guacamole" of material! My education and research ever since my college years have benefited from numerous wonderful collaborators and colleagues listed in Figure 26, and I have truly enjoyed being a student of many of them. I am sure that some have been left out for which I apologize. Of course, I owe a special personal and professional debt to my spectacular mentors, the institutions who have hosted me, and the various funding agencies, administrators, and staff that have supported my work listed on Figure 27. Finally, on Figure 28, I sincerely and deeply thank my family and my close personal friends who have listened to and counseled me through many challenges over the years. My parents sacrificed a great deal for me and provided continuing love and support to me throughout their lives, and I have thoroughly enjoyed the well-wishes and encouragement from all members of my extended family. My son Daniel, an inquisitive and deep thinker, always listens and continues to amaze me, and he provides a continuing inspiration for the future. My wife, Sharon, has been an indispensable source of love, companionship, patience, and encouragement to me throughout our marriage, and I cannot thank her enough.

Thanks to Moerner Lab Alumni!

IBM Almaden Research Ctr., San Jose:

- Dr. Alan Huston
- Dr. Howard Lee
- Dr. Thomas Carter
- Dr. Lothar Kador
- Dr. W. Pat Ambrose
- Prof. Dr. Thomas Basché
- Prof. Anne Myers
- Dr. Paul Tchenio
- Dr. Jürgen Köhler
- Prof. Stephen Ducharme
- Dr. Peggy Walsh
- Dr. John Stankus
- Dr. Scott Silence
- Dr. Constantina Poga
- Dr. Yiwei Jia

University of California, San Diego:

- Ms. Courtney Thompson
- Dr. David J. Norris,
- Dr. Anders Grunnet-Jepsen
- Dr. Susanne Kummer
- Dr. Rob Dickson
- Dr. Maria Diaz-Garcia
- Mr. James Frazier
- Mr. Tim Marsh
- Ms. Julie Casperson
- Ms. Laura Neurauter
- Mr. Barry Smith

Stanford University:

- Dr. Erwin J. G. Peterman
- Dr. Arosha Goonesekera
- Dr. Sophie Brasselet
- Dr. Brahim Lounis
- Mr. Andre Leopold
- Mr. Erik Bjerneld
- Mr. Shaumo Sudhukhan
- Ms. Yeonsuk Roh
- Dr. Ueli Gubler
- Dr. Dan Wright
- Dr. Matt Paige
- Dr. Oksana Ostroverkhova
- Dr. Stephan Hess
- Dr. Marija Vrljic
- Dr. Jason Deich
- Mr. Johann Schleier-Smith
- Dr. Kallie Willets
- Dr. Hans-Philipp Lerch
- Dr. Stefanie Nishimura
- Dr. David P. Fromm
- Dr. P. James Schuck
- Ms. Jennifer Alyono
- Dr. Jaesuk Hwang
- Mr. Kit Werley
- Dr. Hanshin Hwang
- Mr. Naveen Sinha
- Dr. Adam E. Cohen
- Dr. Laurent Coolen

- Dr. Marcelle Koenig
- Dr. Andrea Kurtz
- Dr. So Yeon Kim
- Dr. Frank Jaeckel
- Ms. Nicole Tselentis
- Dr. Magnus Hsu
- Dr. Nick Conley
- Dr. Julie Biteen
- Dr. Sam Lord
- Dr. Shigeki Iwanaga
- Dr. Anika Kinkhabwala
- Dr. Alexandre Fuerstenberg
- Mr. Andrey Andreev
- Dr. Jianwei Liu
- Dr. Steven F. Lee
- Dr. Majid Badieirostami
- Dr. Randall Goldsmith
- Dr. Michael Thompson
- Mr. Alex Chang
- Dr. Hsiao-lu Denise Lee
- Ms. Yao Yue
- Dr. Whitney Duim
- Dr. Yan Jiang
- Ms. Katie Evans
- Dr. Lana Lau
- Dr. Sam Bockenhauer
- Dr. Andreas Gahlmann
- Dr. Steffen Sahl
- Dr. Gabriela Schlau-Cohen
- Dr. Matthew Lew
- Prof. Michael Börsch

FIGURE 24. Moerner lab alumni.

More Thanks: The Current Guacamole Team!

Moerner Group

Dr. Yoav Shechtman
Dr. Saumya Saurabh
Dr. Quan Wang
Dr. Allison Squires
Marissa Lee
Mikael Backlund
Lucien Weiss
Adam Backer
Alex Diezmann
Hsiang-yu Yang
Colin Comerci
Camille Bayas
Josh Yoon
Maurice Lee
Petar Petrov
Jingying Yue (rotator)

Sam Lord

one molecule = one guacamole
(i.e., 1 over Avocado's Number of moles, $1/N_A$ moles)

(with apologies to the memory of Amadeo Avogadro)

FIGURE 25. The Current Guacamole Team!

Thanks to My Collaborators/Colleagues!

Washington University:
- Jan Brown, Harry Ringermacher, Marjorie Yuhas, …

Cornell University
- Yves Chabal, Aland Chin, Andy Chraplyvy, Fred Pinkerton, Eric Schiff, Don Trotter, …

IBM Research:
- Gary C. Bjorklund, Christoph Bräuchle (TU Munich), Don Burland, Bryan Kohler (Wesleyan), Bill Lenth, Marc Levenson, Roger MacFarlane, Chris Moylan, Michel Orrit (CNRS), Jan Schmidt (Leiden), Robert Shelby, Campbell Scott, Robert Twieg, …

ETH Zürich:
- Bert Hecht, Thomas Irngartinger, Viktor Palm, Taras Plakhotnik, Dieter Pohl (IBM), Aleks Rebane, Urs P. Wild, ….

UCSD:
- Larry Goldstein, Jay Siegel, Susan Taylor, Mark Thiemens, Roger Tsien, Bruno Zimm, …

Stanford:
- Thijs Aartsma (Leiden), Steve Boxer, Chris Calderon (Numerica), Gerard Canters (Leiden), Wah Chiu (BCM), Justin DuBois, Shanhui Fan, Gordon Kino, Eric Kool, Harden McConnell, Rafael Peistun (CU), Ljiljana Milenkovic, Matthew Scott, Lucy Shapiro, Andy Spakowitz, Tim Stearns, Bob Waymouth, Karsten Weis (UCB), Paul Wender, and many more

FIGURE 26. Thanks to My Collaborators/Colleagues!

Thanks to My Mentors, Homes, Funding Sources

Mentors:
- High School (Thomas Jefferson): Mrs. Blanche Rodriguez, Dr. Richard G. Domey (Bioengineering, UTMSSA)
- Undergrad (Wash U): James G. Miller
- Graduate (Cornell): Albert J. Sievers III
- Professional:
  - IBM: Gary C. Bjorklund, Dan Auerbach, Jerry Swalen, George Castro, Grant Willson
  - UCSD: Kent Wilson, Katja Lindenberg
  - Stanford: Harden McConnell, Dick Zare, Michael Fayer

JGM '75 AJS '81

Funding: U. S. Agencies: ONR, NSF, NIH-NIGMS, NIH-NEI, DOE-BES

Institutions post PhD:
- IBM Research, San Jose and Almaden Research Centers
- ETH Zurich (Guest Professor of Urs P. Wild)
- The University of California, San Diego, Dept. Chemistry and Biochemistry
- Stanford University, Department of Chemistry
- Administrators and Staff, Administrative Assistants Kathi Robbins, Ann Olive

FIGURE 27. Thanks to My Mentors, Homes, Funding Sources.

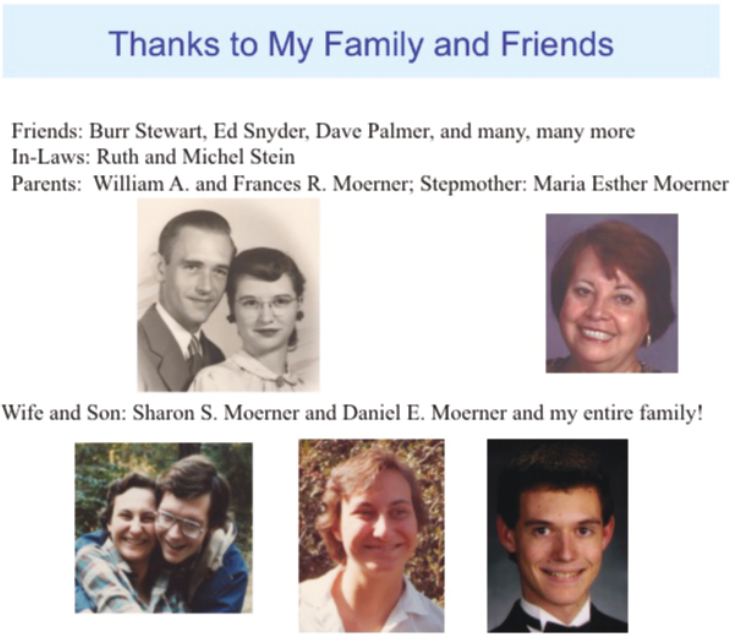

FIGURE 28. Thanks to My Family and Friends.

REFERENCES

1. Moerner WE, Kador L. Optical detection and spectroscopy of single molecules in a solid. *Phys Rev Lett*. 1989; **62**: 2535–2538.
2. Dickson RM, Cubitt AB, Tsien RY, Moerner WE. On/Off blinking and switching behavior of single molecules of green fluorescent protein. *Nature*. 1997; **388**: 355–358.
3. Itano WM, Bergquist JC, Wineland DJ. Laser spectroscopy of trapped atomic ions. *Science*. 1987; **237**: 612.
4. Diedrich F, Krause J, Rempe G, Scully MO, Walther H. Laser experiments with single atoms as A test of basic physics. *IEEE J Quant Elect*. 1988; **24**: 1314.
5. Dehmelt H. Experiments with an isolated subatomic particle at rest. *Rev Mod Phys*. 1990; **62**: 525–530.
6. Binnig G, Rohrer H. Scanning tunneling microscopy-from birth to adolescence. *Rev Mod Phys*. 1987; **59**: 615.
7. Binnig G, Quate CF, Gerber C. Atomic force microscope. *Phys Rev Lett*. 1986; **56**: 930–933.
8. Neher E, Sakmann B. Single-channel currents recorded from membrane of denervated frog muscle fibres. *Nature*. 1976 04/29; **260**(5554): 799–802.
9. Schrödinger ERJA. Are there quantum jumps? part II. *British J Phil Science*. 1952; **3**: 233–242.

10. Pope M, Swenberg CE. Electronic processes in organic crystals and polymers. London: Oxford Univ. Press; 1999.
10½. Kummer S, Kulzer F, Kettner R, Basché T, Tietz C, Glowatz C, Kryschi C, Absorption, excitation, and emission spectroscopy of terrylene in *p*-terphenyl. Bulk measurements and single molecule studies. *J.Chem.Phys.* 1997; **107**:7673–7684.
11. Orlowski TE, Zewail AH. Radiationless relaxation and optical dephasing of molecules excited by wide- and narrow-band lasers. II. pentacene in low-temperature mixed crystals. *J Chem Phys*. 1979; **70**(3): 1390–1426.
12. Stoneham AM. Shapes of inhomogeneously broadened resonance lines in solids. *Rev Mod Phys*. 1969; **41**: 82.
13. Personov RI, Al'Shits EI, Bykovskaya LA. The effect of fine structure appearance in laser-excited fluorescence spectra of organic compounds in solid solutions. *Opt Commun*. 1972 10; **6**(2): 169–173.
14. Orrit M, Bernard J, Personov RI. High-resolution spectroscopy of organic molecules in solids: From fluorescence line narrowing and hole burning to single molecule spectroscopy. *J Phys Chem*. 1993; **97**: 10256–10268.
15. de Vries H, Wiersma DA. Fluorescence transient and optical free induction decay spectroscopy of pentacene in mixed crystals at 2 K. determination of intersystem crossing and internal conversion rates. *J Chem Phys*. 1979; **70**: 5807.
16. Wiersma DA. Coherent optical transient studies of dephasing and relaxation in electronic transitions of large molecules in the condensed phase. *Adv Chem Phys*. 1981; **47**: 421.
17. Berg M, Walsh CA, Narasimhan LR, Littau KA, Fayer MD. Dynamics in low temperature glasses: Theory and experiments on optical dephasing, spectral diffusion, and hydrogen tunneling. *J Chem Phys*. 1988; **88**(3): 1564–1587.
18. Gorokhovskii AA, Kaarli RK, Rebane LA. Hole burning in the contour of a pure electronic line in a Shpol'skii system. *JETP Lett*. 1974; **20**: 216.
19. Kharlamov BM, Personov RI, Bykovskaya LA. Stable "gap" in absorption spectra of solid solutions of organic molecules by laser irradiation. *Opt Commun*. 1974 10; **12**(2): 191–193.
20. Moerner WE. Molecular electronics for frequency domain optical storage: Persistent spectral hole-burning—a review. *J Molec Electr*. 1985; **1**: 55–71.
21. Moerner WE, ed. *Topics in current physics 44; Persistent spectral hole-burning: Science and applications*. Berlin: Springer; 1988.
22. Friedrich J, Haarer D. Photochemical hole burning: A spectroscopic study of relaxation processes in polymers and glasses. *Angewandte Chemie International Edition in English*. 1984; **23**(2): 113–140.
23. Hayes JM, Small GJ. Mechanisms of non-photochemical hole-burning in organic glasses. *Chemical Physics Letters*. 1978 3/15; **54**(3): 435–438.
24. Hayes JM, Small GJ. Non-photochemical hole burning and impurity site relaxation processes in organic glasses. *Chem Phys*. 1978 1/1; **27**(1): 151–157.
25. Babbitt WR, Barber ZW, Bekker SH, Chase MD, Harrington C, Merkel KD, Mohan RK, Sharpe T, Stiffler CR, Traxinger AS, Woidtke AJ. From spectral holeburning memory to spatial-spectral microwave signal processing. *Laser Phys*. 2014; **24**(9): 094002.
26. Moerner WE, Levenson MD. Can single-photon processes provide useful materials for frequency-domain optical storage? *J Opt Soc Am B*. 1985 Jun; **2**(6): 915–924.

27. Moerner WE, Carter TP. Statistical fine structure in inhomogeneously broadened absorption lines. *Phys Rev Lett*. 1987; **59**: 2705.
28. Carter TP, Manavi M, Moerner WE. Statistical fine structure in the inhomogeneously broadened electronic origin of pentacene in *p*-terphenyl. *J Chem Phys*. 1988; **89**: 1768.
29. Bjorklund GC. Frequency-modulation spectroscopy: A new method for measuring weak absorptions and dispersions. *Opt Lett*. 1980; **5**: 15.
30. Carter TP, Horne DE, Moerner WE. Pseudo-stark effect and FM/Stark double-modulation spectroscopy for the detection of statistical fine structure in alexandrite. *Chem Phys Lett*. 1988; **151**: 102.
31. Bjorklund GC, Levenson MD, Lenth W, Ortiz C. Frequency modulation (FM) spectroscopy. *Appl Phys B*. 1983; **32**: 145.
32. Kador L, Horne DE, Moerner WE. Optical detection and probing of single dopant molecules of pentacene in a *p*-terphenyl host crystal by means of absorption spectroscopy. *J Phys Chem*. 1990; **94**: 1237–1248.
33. Whittaker EA, Gehrtz M, Bjorklund GC. Residual amplitude modulation in laser electro-optic phase modulation. *J Opt Soc Am B*. 1985; **2**: 1320.
34. Kador L, Latychevskaia T, Renn A, Wild UP. Absorption spectroscopy on single molecules in solids. *J Chem Phys*. 1999; **111**: 8755–8758.
35. Orrit M, Bernard J. Single pentacene molecules detected by fluorescence excitation in a *p*-terphenyl crystal. *Phys Rev Lett*. 1990; **65**: 2716–2719.
36. Tango WJ, Link JK, Zare RN. Spectroscopy of K_2 using laser-induced fluorescence. *J Chem Phys*. 1968; **49**(10): 4264–4268.
37. Orrit M, Bernard J, Zumbusch A, Personov RI. Stark effect on single molecules in a polymer matrix. *Chem Phys Lett*. 1992; **196**: 595.
38. Zumbusch A, Fleury L, Brown R, Bernard J, Orrit M. Probing individual two-level systems in a polymer by correlation of single-molecule fluorescence. *Phys Rev Lett*. 1993; **70**: 3584–3587.
39. Güttler F, Croci M, Renn A, Wild UP. Single molecule polarization spectroscopy: Pentacene in *p*-terphenyl. *Chem Phys*. 1996; **211**(1): 421–430.
40. Basché T, Moerner WE, Orrit M, Wild UP, editors. *Single molecule optical detection, imaging, and spectroscopy*. Munich: Verlag-Chemie; 1997.
41. Moerner WE, Basché T. Optical spectroscopy of single impurity molecules in solids. *Angew Chem Int Ed*. 1993; **105**: 537.
42. Moerner WE, Dickson RM, Norris DJ. Single-molecule spectroscopy and quantum optics in solids. *Adv Atom Molec Opt Phys*. 1997; **38**: 193–236.
43. Skinner JL, Moerner WE. Structure and dynamics in solids as probed by optical spectroscopy. *J Phys Chem*. 1996; **100**: 13251–13262.
44. Moerner WE. High-resolution optical spectroscopy of single molecules in solids. *Acc Chem Res*. 1996; **29**: 563.
45. Moerner WE. Examining nanoenvironments in solids on the scale of a single, isolated molecule. *Science*. 1994; **265**: 46–53.
46. Orrit M, Bernard J, Brown R, Lounis B. Optical spectroscopy of single molecules in solids. *Prog Optics*. 1996; **35**: 61–144.
47. Plakhotnik T, Donley EA, Wild UP. Single-molecule spectroscopy. *Annu Rev Phys Chem*. 1996; **48**: 181–212.
48. Ambrose WP, Moerner WE. Fluorescence spectroscopy and spectral diffusion of single impurity molecules in a crystal. *Nature*. 1991; **349**: 225–227.

49. Ambrose WP, Basché T, Moerner WE. Detection and spectroscopy of single pentacene molecules in a *p*-terphenyl crystal by means of fluorescence excitation. *J Chem Phys*. 1991; **95**: 7150–7163.
50. Basché T, Moerner WE, Orrit M, Talon H. Photon antibunching in the fluorescence of a single dye molecule trapped in a solid. *Phys Rev Lett*. 1992; **69**: 1516–1519.
51. Tchénio P, Myers AB, Moerner WE. Dispersed fluorescence spectra of single molecules of pentacene in *p*-terphenyl. *J Phys Chem*. 1993; **97**: 2491.
52. Tchénio P, Myers AB, Moerner WE. Vibrational analysis of dispersed fluorescence from single molecules of terrylene in polyethylene. *Chem Phys Lett*. 1993; **213**: 325.
53. Myers AB, Tchénio P, Zgierski M, Moerner WE. Vibronic spectroscopy of individual molecules in solids. *J Phys Chem*. 1994; **98**: 10377.
54. Köhler J, Disselhorst JAJM, Donckers MCJM, Groenen EJJ, Schmidt J, Moerner WE. Magnetic resonance of a single molecular spin. *Nature*. 1993; **363**: 242–244.
55. Moerner WE, Plakhotnik T, Irngartinger T, Wild UP, Pohl D, Hecht B. Near-field optical spectroscopy of individual molecules in solids. *Phys Rev Lett*. 1994; **73**: 2764.
56. Moerner WE, Ambrose WP. Comment on "Single pentacene molecules detected by fluorescence excitation in a *p*-terphenyl crystal." *Phys Rev Lett*. 1991; **66**: 1376.
57. Patterson FG, Lee HWH, Wilson WL, Fayer MD. Intersystem crossing from singlet states of molecular dimers and monomers in mixed molecular crystals: Picosecond stimulated photon echo experiments. *Chem Phys*. 1984; **84**: 51.
58. Güttler F, Irngartinger T, Plakhotnik T, Renn A, Wild UP. Fluorescence microscopy of single molecules. *Chem Phys Lett*. 1994; **217**: 393.
59. Friedrich J, Haarer D. Structural relaxation processes in polymers and glasses as studied by high resolution optical spectroscopy. In: Zschokke I, editor. *Optical Spectroscopy of Glasses*. Dordrecht: Reidel; 1986. p. 149.
60. Reilly PD, Skinner JL. Spectral diffusion of single molecule fluorescence: A probe of low-frequency localized excitations in disordered crystals. *Phys Rev Lett*. 1993; **71**: 4257–4260.
61. Reilly PD, Skinner JL. Spectral diffusion of individual pentacene molecules in *p*-terphenyl crystal: Stochastic theoretical model and analysis of experimental data. *J Chem Phys*. 1995; **102**: 1540.
62. Geva E, Skinner JL. Theory of single-molecule optical line-shape distributions in low-temperature glasses. *J Phys Chem B*. 1997; **101**: 8920–8932.
63. Plakhotnik T, Moerner WE, Irngartinger T, Wild UP. Single-molecule spectroscopy in shpol'skii matrices. *Chimia*. 1994; **48**: 31.
64. Basché T, Moerner WE. Optical modification of a single impurity molecule in a solid. *Nature*. 1992; **355**: 335–337.
65. Basché T, Ambrose WP, Moerner WE. Optical spectra and kinetics of single impurity molecules in a polymer: Spectral diffusion and persistent spectral hole-burning. *J Opt Soc Am B*. 1992; **9**: 829.
66. Tchénio P, Myers AB, Moerner WE. Optical studies of single terrylene molecules in polyethylene. *J Lumin*. 1993; **56**: 1.
67. Moerner WE, Plakhotnik T, Irngartinger T, Croci M, Palm V, Wild UP. Optical probing of single molecules of terrylene in a Shpolskii matrix—A two-state single-molecule switch. *J Phys Chem*. 1994; **98**: 7382–7389.

68. Ha T, Enderle T, Ogletree DF, Chemla DS, Selvin PR, Weiss S. Probing the interaction between two single molecules: Fluorescence resonance energy transfer between a single donor and a single acceptor. *Proc Natl Acad Sci U S A*. 1996; **93**: 6264–6268.
69. Moerner WE, Schuck PJ, Fromm DP, Kinkhabwala A, Lord SJ, Nishimura SY, Willets KA, Sundaramurthy A, Kino GS, He M, Lu Z, Twieg RJ. Nanophotonics and single molecules. In: Rigler R, Vogel H, editors. *Single Molecules and Nanotechnology*. Berlin: Springer-Verlag; 2008. p. 1–23.
70. Kinkhabwala A, Yu Z, Fan S, Avlasevich Y, Mullen K, Moerner WE. Large single-molecule fluorescence enhancements produced by a gold bowtie nanoantenna. *Nature Photon*. 2009; **3**: 654.
71. Magde D, Elson E, Webb WW. Thermodynamic flucutations in a reacting system—measurement by fluorescence correlation spectroscopy. *Phys Rev Lett*. 1972; **28**: 705.
72. Elson EL, Magde D. Fluorescence correlation spectroscopy. I. conceptual basis and theory. *Biopolymers*. 1974; **13**: 1–27.
73. Magde DL, Elson EL, Webb WW. Fluorescence correlation spectroscopy. II. an experimental realization. *Biopolymers*. 1974; **13**: 29–61.
74. Magde D, Webb WW, Elson EL. Fluorescence correlation spectroscopy. III. uniform translation and laminar flow. *Biopolymers*. 1978; **17**: 361–367.
75. Ehrenberg M, Rigler R. Rotational brownian motion and fluorescence intensify fluctuations. *Chem Phys*. 1974 /6; **4**(3): 390–401.
76. Aragón SR, Pecora R. Fluorescence correlation spectroscopy as a probe of molecular dynamics. *J Chem Phys*. 1976; **64**(4): 1791–1803.
77. Rigler R, Widengren J. Ultrasensitive detection of single molecules by fluorescence correlation spectroscopy. In: Klinge B, Owman C, editors. *Bioscience third conference*; 1990; Lund, Sweden: Lund University Press; 1990. p. 180–183.
78. Peck K, Stryer L, Glazer AN, Mathies RA. Single-molecule fluorescence detection—auto-correlation criterion and experimental realization with phycoerythrin. *Proc Natl Acad Sci U S A*. 1989; **86**(11): 4087–4091.
79. Shera EB, Seitzinger NK, Davis LM, Keller RA, Soper SA. Detection of single fluorescent molecules. *Chem Phys Lett*. 1990; **174**: 553–557.
80. Nie S, Chiu DT, Zare RN. Probing individual molecules with confocal fluorescence microscopy. *Science*. 1994; **266**: 1018–1021.
81. Hirschfeld T. Optical microscopic observation of single small molecules. *Appl Opt*. 1976 12/01; **15**(12): 2965–2966.
82. Betzig E, Chichester RJ. Single molecules observed by near-field scanning optical microscopy. *Science*. 1993; **262**: 1422–1425.
83. Ambrose WP, Goodwin PM, Martin JC, Keller RA. Single-molecule detection and photochemistry on a surface using near-field optical-excitation. *Phys Rev Lett*. 1994; **72**: 160–163.
84. Xie XS, Dunn RC. Probing single-molecule dynamics. *Science*. 1994; **265**: 361–364.
85. Macklin JJ, Trautman JK, Harris TD, Brus LE. Imaging and time-resolved spectroscopy of single molecules at an interface. *Science*. 1996; **272**: 255–258.
86. Funatsu T, Harada Y, Tokunaga M, Saito K, Yanagida T. Imaging of single fluorescent molecules and individual ATP turnovers by single myosin molecules in aqueous solution. *Nature*. 1995; **374**: 555–559.

87. Schmidt T, Schutz GJ, Baumgartner W, Gruber HJ, Schindler H. Imaging of single molecule diffusion. *Proc Natl Acad Sci U S A*. 1996; **93**: 2926–2929.
88. Rigler R, Elson E, editors. *Fluorescence correlation spectroscopy*. Berlin: Springer; 2001.
89. Schwille P. Fluorescence correlation spectroscopy and its potential for intracellular applications. *Cell Biochem Biophys*. 2001; **34**(3): 383–408.
90. Hess ST, Huang S, Heikal AA, Webb WW. Biological and chemical applications of fluorescence correlation spectroscopy: A review. *Biochemistry*. 2002; **41**(3): 697–705.
91. Weiss S. Fluorescence spectroscopy of single biomolecules. *Science*. 1999; **283**: 1676–1683.
92. Moerner WE, Orrit M. Illuminating single molecules in condensed matter. *Science*. 1999; **283**: 1670–1676.
93. Moerner WE. Single-molecule optical spectroscopy and imaging: From early steps to recent advances. In: Graslund A, Rigler R, Widengren J, editors. *Single Molecule Spectroscopy in Chemistry, Physics and Biology*: Nobel Symposium 138 Proceedings. Berlin: Springer-Verlag; 2010. p. 25–60.
94. Rigler R, Orrit M, Basche T, editors. *Single molecule spectroscopy*: Nobel conference lectures. Berlin: Springer-Verlag; 2001.
95. Gräslund A, Rigler R, Widengren J, editors. *Single molecule spectroscopy in chemistry, physics and biology*: Nobel symposium 138 proceedings. Berlin: Springer-Verlag; 2010.
96. Zander C, Enderlein J, Keller RA. *Single-molecule detection in solution: Methods and applications*. Berlin: Wiley-VCH; 2002.
97. Gell C, Brockwell DJ, Smith A. *Handbook of single molecule fluorescence spectroscopy*. Oxford: Oxford Univ. Press; 2006.
98. Selvin PR, Ha T, editors. *Single-molecule techniques: A laboratory manual*. Cold Spring Harbor, NY: Cold Spring Harbor Laboratory Press; 2008.
99. Hinterdorfer P, van Oijen AM, editors. *Handbook of single-molecule biophysics*. New York: Springer; 2009.
99½. Moerner WE, Fromm DP, Methods of single-molecule fluorescence spectroscopy and microscopy. *Rev. Sci. Instrum.* 2003; **74**: 3597–3619.
100. Vrljic M, Nishimura SY, Brasselet S, Moerner WE, McConnell HM. Translational diffusion of individual class II MHC membrane proteins in cells. *Biophys J*. 2002; **83**: 2681–2692. PMCID: PMC1302352.
101. Vrljic M, Nishimura SY, Moerner WE, McConnell HM. Cholesterol depletion suppresses the translational diffusion of class II major histocompatibility complex proteins in the plasma membrane. *Biophys J*. 2005; **88**: 334–347.
102. Nishimura S, Vrljic M, Klein LO, McConnell HM, Moerner WE. Cholesterol depletion induces solid-like regions in the plasma membrane. *Biophys J*. 2006; **90**: 927–938. PMCID: PMC1367117.
103. Vrljic M, Nishimura SY, Moerner WE. Single-molecule tracking. *Methods Mol Biol*. 2007; **398**: 193–219.
104. Werley CA, Moerner WE. Single-molecule nanoprobes explore defects in spin-grown crystals. *J Phys Chem B*. 2006; **110**: 18939–18944.

105. Dickson RM, Norris DJ, Moerner WE. Simultaneous imaging of individual molecules aligned both parallel and perpendicular to the optic axis. *Phys Rev Lett*. 1998; **81**: 5322–5325.

105½. Deich J, Judd EM, McAdams HH, Moerner WE, Visualization of the movement of single histidine kinase molecules in live Caulobacter cells, *Proc. Nat. Acad. Sci. (USA)* 2004; **101:** 15921–15926.

106. Shapiro L, McAdams H, Losick R. Generating and exploiting polarity in bacteria. *Science*. 2002; **298**: 1942–1946.

107. Goley ED, Iniesta AA, Shapiro L. Cell cycle regulation in *Caulobacter*: Location, location, location. *J Cell Sciences*. 2007; **120**: 3501–3507.

108. Kim SY, Gitai Z, Kinkhabwala A, Shapiro L, Moerner WE. Single molecules of the bacterial actin MreB undergo directed treadmilling motion in *Caulobacter crescentus*. *Proc Natl Acad Sci U S A*. 2006; **103**(29): 10929–10934. PMCID: PMC1544151.

109. van Teeffelen S, Wang S, Furchtgott L, Huang KC, Wingreen NS, Shaevitz JW, Gitai Z. The bacterial actin MreB rotates, and rotation depends on cell-wall assembly. *Proc Natl Acad Sci U S A*. 2011 SEP 20; **108**(38): 15822–15827.

110. Abbe E. Contributions to the theory of the microscope and microscopic detection (translated from German). *Arch Mikroskop Anat*. 1873; **9**: 413–468.

111. Hell SW, Wichmann J. Breaking the diffraction resolution limit by stimulated emission: Stimulated-emission-depletion fluorescence microscopy. *Opt Lett*. 1994; **19**: 780–782.

112. Gustafsson MGL. Surpassing the lateral resolution limit by a factor of two using structured illumination microscopy. *J Microsc*. 2000; **198**(2): 82–87.

113. Backlund MP, Lew MD, Backer A. S., Sahl SJ, Moerner WE. The role of molecular dipole orientation in single-molecule fluorescence microscopy and implications for super-resolution imaging. *Chem Phys Chem*. 2014; **15**: 587–599.

114. Betzig E, Patterson GH, Sougrat R, Lindwasser OW, Olenych S, Bonifacino JS, Davidson MW, Lippincott-Schwartz J, Hess HF. Imaging intracellular fluorescent proteins at nanometer resolution. *Science*. 2006; **313**(5793): 1642–1645.

115. Thompson RE, Larson DR, Webb WW. Precise nanometer localization analysis for individual fluorescent probes. *Biophys J*. 2002; **82**(5): 2775–2783.

116. Michalet X, Weiss S. Using photon statistics to boost microscopy resolution. *Proc Natl Acad Sci U S A*. 2006; **103**: 4797–4798.

117. Mortensen KI, Churchman LS, Spudich JA, Flyvbjerg H. Optimized localization analysis for single-molecule tracking and super-resolution microscopy. *Nat Methods*. 2010; **7**(5): 377–381.

118. Barak LS, Webb WW. Diffusion of low density lipoprotein-receptor complex on human fibroblasts. *J Cell Biol*. 1982; **95**: 846–852.

119. Gelles J, Schnapp BJ, Sheetz MP. Tracking kinesin-driven movements with nanometre-scale precision. *Nature*. 1988; **4**: 450–453.

120. Seisenberger G, Ried MU, Endress T, Buning H, Hallek M, Braeuchle C. Real-time single-molecule imaging of the infection pathway of an adeno-associated virus. *Science*. 2001; **294**: 1929–1932.

121. Bobroff N. Position measurement with a resolution and noise-limited instrument. *Rev Sci Instrum*. 1986; **57**: 1152–1157.

122. Heisenberg W. *The Physical Principles of Quantum Theory*. Chicago: University of Chicago Press; 1930. p. 22.
123. Yildiz A, Forkey JN, McKinney SA, Ha T, Goldman YE, Selvin PR. Myosin V walks hand-over-hand: Single fluorophore imaging with 1.5-nm localization. *Science*. 2003; **300**: 2061–2065.
124. Tsien RY. The green fluorescent protein. *Annu Rev Biochem*. 1998; **67**: 509–544.
125. Dickson RM, Norris DJ, Tzeng YL, Moerner WE. Three-dimensional imaging of single molecules solvated in pores of poly(acrylamide) gels. *Science*. 1996; **274**(5289): 966–969.
126. Chattoraj M, King BA, Bublitz GU, Boxer SG. Ultra-fast excited state dynamics in green fluorescent protein: Multiple states and proton transfer. *Proc Natl Acad Sci U S A*. 1996; **93**: 8362–8367.
127. Ando R, Hama H, Yamamoto-Hino M, Mizuno H, Miyawaki A. An optical marker based on the UV-induced green-to-red photoconversion of a fluorescent protein. *Proc Natl Acad Sci U S A*. 2002; **99**: 12651–12656.
128. Patterson GH, Lippincott-Schwartz J. A photoactivatable GFP for selective photolabeling of proteins and cells. *Science*. 2002; **297**: 1873–1877.
129. Wiedenmann J, Ivanchenko S, Oswald F, Schmitt F, Röcker C, Salih A, Spindler K, Nienhaus GU. EosFP, a fluorescent marker protein with UV-inducible green-to-red fluorescence conversion. *Proc Natl Acad Sci U S A*. 2004 November 9; **101**(45): 15905–15910.
130. Ando R, Mizuno H, Miyawaki A. Regulated fast nucleocytoplasmic shuttling observed by reversible protein highlighting. *Science*. 2004; **306**: 1370–1373.
131. Betzig E. Proposed method for molecular optical imaging. *Opt Lett*. 1995; **20**(3): 237–239.
132. van Oijen AM, Köhler J, Schmidt J, Müller M, Brakenhoff GJ. 3-dimensional super-resolution by spectrally selective imaging. *Chem Phys Lett*. 1998; **292**: 183–187.
133. van Oijen AM, Köhler J, Schmidt J, Müller M, Brakenhoff GJ. Far-field fluorescence microscopy beyond the diffraction limit. *J Opt Soc Am A*. 1999; **16**: 909–915.
133½. Lacoste TD, Michalet X, Pinaud F, Chemla DS, Alivisatos AP, Weiss S, Ultrahigh-resolution multicolor colocalization of single fluorescent probes. *Proc. Nat. Acad. Sci. (USA)*. 2000, **97:** 9461–9466.
134. Heilemann M, Herten DP, Heintzmann R, Cremer C, Müller C, Tinnefeld P, Weston KD, Wolfrum J, Sauer M. High-resolution colocalization of single dye molecules by fluorescence lifetime imaging microscopy. *Anal Chem*. 2002 07/01; 2015/01; **74**(14): 3511–3517.
135. Gordon MP, Ha T, Selvin PR. Single-molecule high-resolution imaging with photobleaching. *Proc Natl Acad Sci U S A*. 2004; **101**: 6462–6465.
136. Qu X, Wu D, Mets L, Scherer NF. Nanometer-localized multiple single-molecule fluorescence microscopy. *Proc Natl Acad Sci U S A*. 2004; **101**: 11298–11303.
137. Churchman LS, Oekten Z, Rock RS, Dawson JF, Spudich JA. Single molecule high-resolution colocalization of Cy3 and Cy5 attached to macromolecules measures intramolecular distances through time. *Proc Natl Acad Sci U S A*. 2005; **102**(5): 1419–1423.
138. Lidke KA, Rieger B, Jovin TM, Heintzmann R. Superresolution by localization of quantum dots using blinking statistics. *Opt Express*. 2005; **13**: 7052–7062.
139. Moerner WE. New directions in single-molecule imaging and analysis. *Proc Natl Acad Sci U S A*. 2007; **104**: 12596–12602.

140. Churchman LS, Flyvbjerg H, Spudich JA. A non-gaussian distribution quantifies distances measured with fluorescence localization techniques. *Biophys J*. 2006; **90**: 668–671.
141. Rust MJ, Bates M, Zhuang X. Sub-diffraction-limit imaging by stochastic optical reconstruction microscopy (STORM). *Nat Methods*. 2006; **3**(10): 793–796.
142. Hess ST, Girirajan TPK, Mason MD. Ultra-high resolution imaging by fluorescence photoactivation localization microscopy. *Biophys J*. 2006; **91**(11): 4258–4272.
143. Sharonov A, Hochstrasser RM. Wide-field subdiffraction imaging by accumulated binding of diffusing probes. *Proc Natl Acad Sci U S A*. 2006; **103**(50): 18911–18916.
144. Mei E, Gao F, Hochstrasser RM. Controlled biomolecular collisions allow sub-diffraction limited microscopy of lipid vesicles. *Phys Chem Chem Phys*. 2006; **8**: 2077–2082.
145. Heilemann M, van de Linde S, Schüttpelz M, Kasper R, Seefeldt B, Mukherjee A, Tinnefeld P, Sauer M. Subdiffraction-resolution fluorescence imaging with conventional fluorescent probes. *Angew Chem Int Ed*. 2008; **47**(33): 6172–6176.
146. Testa I, Wurm CA, Medda R, Rothermel E, von Middendorf C, Foelling J, Jakobs S, Schoenle A, Hell SW, Eggeling C. Multicolor fluorescence nanoscopy in fixed and living cells by exciting conventional fluorophores with a single wavelength. *Biophys J*. 2010; **99**(8): 2686–2694.
147. Cordes T, Strackharn M, Stahl SW, Summerer W, Steinhauer C, Forthmann C, Puchner EM, Vogelsang J, Gaub HE, Tinnefeld P. Resolving single-molecule assembled patterns with superresolution blink-microscopy. *Nano Lett*. 2010; **10**(2): 645–651.
148. Lemmer P, Gunkel M, Baddeley D, Kaufmann R, Urich A, Weiland Y, Reymann J, Mueller P, Hausmann M, Cremer C. SPDM: Light microscopy with single-molecule resolution at the nanoscale. *Appl Phys B*. 2008 10/01; **93**(1): 1–12.
149. Biteen JS, Thompson MA, Tselentis NK, Bowman GR, Shapiro L, Moerner WE. Super-resolution imaging in live *Caulobacter crescentus* cells using photoswitchable EYFP. *Nat Methods*. 2008; **5**(11): 947–949.
150. Lee HD, Lord SJ, Iwanaga S, Zhan K, Xie H, Williams JC, Wang H, Bowman GR, Goley ED, Shapiro L, Twieg RJ, Rao J, Moerner WE. Superresolution imaging of targeted proteins in fixed and living cells using photoactivatable organic fluorophores. *J Am Chem Soc*. 2010; **132**(43): 15099–15101.
151. Lee MK, Williams J, Twieg RJ, Rao J, Moerner WE. Enzymatic activation of nitroaryl fluorogens in live bacterial cells for enzymatic turnover-activated localization microscopy. *Chem. Sci*. 2013; **4**(1): 220–225.
152. Huang F, Hartwich TMP, Rivera-Molina FE, Lin Y, Duim WC, Long JJ, Uchil PD, Myers JR, Baird MA, Mothes W, Davidson MW, Toomre D, Bewersdorf J. Video-rate nanoscopy using sCMOS camera-specific single-molecule localization algorithms. *Nat. Methods*. 2013; **10**(7): 653–658.
153. Huang B, Babcock H, Zhuang X. Breaking the diffraction barrier: Super-resolution imaging of cells. *Cell*. 2010; **143**: 1047–1058.
154. Thompson MA, Lew MD, Moerner WE. Extending microscopic resolution with single-molecule imaging and active control. *Annu Rev Biophys*. 2012; **41**(1): 321–342.
155. Thompson MA, Biteen JS, Lord SJ, Conley NR, Moerner WE. Molecules and methods for super-resolution imaging. *Meth Enzymol*. 2010; 475: 27–59.

156. Biteen JS, Moerner WE. Single-molecule and superresolution imaging in live bacteria cells. *Cold Spring Harb Perspect Biol*. 2010; 2: a000448.
157. Lew MD, Lee SF, Thompson MA, Lee HD, Moerner WE. Single-molecule photocontrol and nanoscopy. In: Tinnefeld, P. et al. (eds.), *Far-field Optical Nanoscopy. Springer Series on Fluorescence*. Springer Berlin Heidelberg; 2012. p. 1–24.
158. Moerner WE. Microscopy beyond the diffraction limit using actively controlled single molecules. *J Microsc*. 2012; **246**(3): 213–220.
159. Gahlmann A, Ptacin JL, Grover G, Quirin S, von Diezmann ARS, Lee MK, Backlund MP, Shapiro L, Piestun R, Moerner WE. Quantitative multicolor subdiffraction imaging of bacterial protein ultrastructures in 3D. *Nano Lett*. 2013; **13**: 987–993.
160. Sahl SJ, Moerner WE. Super-resolution fluorescence imaging with single molecules. *Curr Opin Struct Biol*. 2013; **23**(5): 778–787.
161. Godin A, Lounis B, Cognet L. Super-resolution microscopy approaches for live cell imaging. *Biophys J*. 2014 10/21; **107**(8): 1777–1784.
162. Swulius MT, Jensen GJ. The helical MreB cytoskeleton in *Escherichia coli* MC1000/pLE7 is an artifact of the N-terminal yellow fluorescent protein tag. *J Bacteriol*. 2012 DEC; **194**(23): 6382–6386.
163. Ptacin JL, Lee SF, Garner EC, Toro E, Eckart M, Comolli LR, Moerner WE, Shapiro L. A spindle-like apparatus guides bacterial chromosome segregation. *Nat Cell Biol*. 2010; **12**(8): 791–798.
164. Lee SF, Thompson MA, Schwartz MA, Shapiro L, Moerner WE. Super-resolution imaging of the nucleoid–associated protein HU in *Caulobacter crescentus*. *Biophys J*. 2011; **100**(7): L31–L33.
165. Coltharp C, Xiao J. Superresolution microscopy for microbiology. *Cell Microbiol*. 2012 DEC 2012; **14**(12): 1808–1818.
166. Gahlmann A, Moerner WE. Exploring bacterial cell biology with single-molecule tracking and super-resolution imaging. *Nat Rev Micro*. 2014; **12**(1): 9–22.
167. Cattoni DI, Fiche JB, Nöllmann M. Single-molecule super-resolution imaging in bacteria. *Curr Opin Microbiol*. 2012 12; **15**(6): 758–763.
168. Ondrus AE, Lee HD, Iwanaga S, Parsons WH, Andresen BM, Moerner WE, Du Bois J. Fluorescent saxitoxins for live cell imaging of single voltage-gated sodium ion channels beyond the optical diffraction limit. *Chem Biol*. 2012; **19**(7): 902–912.
169. Duim WC, Chen B, Frydman J, Moerner WE. Sub-diffraction imaging of huntingtin protein aggregates by fluorescence blink-microscopy and atomic force microscopy. *Chem Phys Chem*. 2011; **12**(13): 2387–2390.
170. Duim WC. *Single-molecule fluorescence and super-resolution imaging of Huntington's disease protein aggregates* [dissertation]. Stanford, CA: Stanford University; 2012.
171. Sahl SJ, Weiss LE, Duim WC, Frydman J, Moerner WE. Cellular inclusion bodies of mutant huntingtin exon 1 obscure small fibrillar aggregate species. *Sci Rep*. 2012; **2**(895): 1–7.
172. Lee MK, Rai P, Williams J, Twieg RJ, Moerner WE. Small-molecule labeling of live cell surfaces for three-dimensional super-resolution microscopy. *J Am Chem Soc*. 2014 10/08; 2015/01; **136**(40): 14003–14006.
173. Huang B, Wang W, Bates M, Zhuang X. Three-dimensional super-resolution imaging by stochastic optical reconstruction microscopy. *Science*. 2008; **319**(5864): 810–813.

174. Ram S, Prabhat P, Chao J, Ward ES, Ober RJ. High accuracy 3D quantum dot tracking with multifocal plane microscopy for the study of fast intracellular dynamics in live cells. *Biophys J*. 2008; **95**(12): 6025–6043.
175. Juette MF, Gould TJ, Lessard MD, Mlodzianoski MJ, Nagpure BS, Bennett BT, Hess ST, Bewersdorf J. Three-dimensional sub-100 nm resolution fluorescence microscopy of thick samples. *Nat Methods*. 2008; **5**(6): 527–529.
176. Backer AS, Moerner WE. Extending single-molecule microscopy using optical Fourier processing. *J Phys Chem B*. 2014; **118**(28): 8313–8329.
177. Pavani SRP, Thompson MA, Biteen JS, Lord SJ, Liu N, Twieg RJ, Piestun R, Moerner WE. Three-dimensional, single-molecule fluorescence imaging beyond the diffraction limit by using a double-helix point spread function. *Proc Natl Acad Sci U S A*. 2009; **106**(9): 2995–2999.
178. Badieirostami M, Lew MD, Thompson MA, Moerner WE. Three-dimensional localization precision of the double-helix point spread function versus astigmatism and biplane. *Appl Phys Lett*. 2010; **97**(16): 161103.
179. Lew MD, Lee SF, Ptacin JL, Lee MK, Twieg RJ, Shapiro L, Moerner WE. Three-dimensional superresolution colocalization of intracellular protein superstructures and the cell surface in live Caulobacter crescentus. *Proc Natl Acad Sci U S A*. 2011; **108**(46): E1102–E1110.
180. Lew MD, Lee SF, Badieirostami M, Moerner WE. Corkscrew point spread function for far-field three-dimensional nanoscale localization of pointlike objects. *Opt Lett*. 2011; **36**(2): 202–204.
181. Backer AS, Backlund MP, Diezmann AR, Sahl SJ, Moerner WE. A bisected pupil for studying single-molecule orientational dynamics and its application to 3D super-resolution microscopy. *Appl Phys Lett*. 2014; **104**(19): 193701-1-193701-5.
182. Shechtman Y, Sahl SJ, Backer AS, Moerner W. Optimal point spread function design for 3D imaging. *Phys Rev Lett*. 2014; **113**(13): 133902.
183. Xu K, Zhong G, Zhuang X. Actin, spectrin, and associated proteins form a periodic cytoskeletal structure in axons. *Science*. 2013 JAN 25; **339**(6118): 452–456.
184. Kusumi A, Tsunoyama TA, Hirosawa KM, Kasai RS, Fujiwara TK. Tracking single molecules at work in living cells. *Nat Chem Biol*. 2014; **10**: 524.
185. Roy R, Hohng S, Ha T. A practical guide to single-molecule FRET. *Nat Methods*. 2008; **5**: 507–516.
186. Grecco HE, Verveer PJ. FRET in cell biology: Still shining in the age of super-resolution? *Chem Phys Chem*. 2011; **12**(3): 484–490.
187. Wang Q, Goldsmith RH, Jiang Y, Bockenhauer SD, Moerner WE. Probing single biomolecules in solution using the anti-brownian electrokinetic (ABEL) trap. *Acc Chem Res*. 2012; **45**: 1955–1964.
188. Schlau-Cohen GS, Bockenhauer S, Wang Q, Moerner WE. Single-molecule spectroscopy of photosynthetic proteins in solution: Exploration of structure–function relationships. *Chem Sci*. 2014; **5**: 2933–2939.
189. Xie XS. Enzyme kinetics, past and present. *Science*. 2013 December 20; **342**(6165): 1457–1459.

Portrait photo of William Esco (W. E.) Moerner by photographer Alexander Mahmoud.